DOE/ET/28389-1
Distribution Category: UC66a

FINAL REPORT

Subsurface Investigations at the Roosevelt KGRA, Utah

Prepared by

Mr. James Butz
Dr. Myron Plooster

University of Denver
Denver Research Institute
P.O. Box 10127
Denver, Colorado 80210

October, 1979

Contract No. DE-AS-08-77ET28389

Prepared for

Department of Energy
Division of Geothermal Energy
Nevada Operations Office

DOE Program Manager: Mr. Joseph Fiore

UNIVERSITY OF DENVER • DENVER RESEARCH INSTITUTE
COLORADO SEMINARY

TABLE OF CONTENTS

LIST OF FIGURES

LIST OF TABLES

ABSTRACT

The Denver Research Institute has carried out an investigation of the geothermal reservoir in the Roosevelt Hot Springs Known Geothermal Resource Area in Utah. The objective of this effort was to develop predictions for well production capacities, based on data taken during field tests and through use of a computer model. In turn, the production information could then be used in design optimization and economic analyses for development of the resource under study.

Flow tests of a geothermal well, "Utah State" 14-2, were conducted in 1978 and 1979. This well is owned jointly by Thermal Power Company, AMAX Exploration, and O'Brien Resources and was operated by Thermal Power. Data consisting of pressure and temperature logs as a function of depth were obtained. Maximum recorded temperature was 503°F (262°C) and maximum pressure, 954 psia (6.58MPa) as measured under flow conditions. Tests were run at rates up to 580,000 lb/hr (73.3 kg/sec) total flow.

The information gathered during the testing was reduced and compared to results of a predictive computer model. Reservoir conditions in the Roosevelt Hot Springs KGRA are such that two-phase flow exists in the wellbore and, in some cases, also in the reservoir itself. The computer model employed in the analysis reflects current efforts to improve the state-of-the-art in the prediction of two-phase pressure drops in vertical systems. Predictions at flowrates of up to 300,000 lb/hr. (38 kg/sec) matched quite well with test data; while modeling at higher flowrates (to maximum tested) showed progressively greater deviation from test data. Cause of the observed degradation is postulated to be the movement of the flash horizon into the reservoir, due to drawdown at high flowrates.

In addition to the comparison with test data, the model was used to develop a parametric data set. From this information an indication of the effects of changes in casing diameter and productivity index on maximum total mass flowrate was developed. For example, by increasing casing diameter to 13 3/8" (34 cm) from existing 9 5/8" (24.4 cm) flowrate can be increased by 24% while maintaining a fixed wellhead pressure of 100 psia (689 kPa). Results show that both parameters can have a significant impact on the maximum flowrate, and therefore on the number of wells needed for a given development strategy.

I. INTRODUCTION

A geothermal well produced in a naturally flashing, two-phase flow mode exhibits markedly different pressure drop behavior in the wellbore than a similar well produced in a single-phase (all-liquid) mode. Phase change from liquid to gas affects the pressure drop in one way due to the vast difference in density of the steam and liquid water components. The temperature is also lowered during the phase change process, as sensible heat is exchanged for latent heat of vaporization. The controlling mechanism for the phase change process is provided by an adherence to the water saturation pressure/temperature curve.

The result of the above considerations in a two-phase flow system is that simply increasing pipe diameter does not necessarily decrease pressure drop in the wellbore, as would be the case in a single phase well. That is to say, there is a minimum and maximum two-phase flow that can be maintained in a pipe of a given diameter, and these values can be significantly greater or less that single-phase flow in an identical sized well. By using predictive tools whose validity has been confirmed, the wells in a geothermal field can therefore be designed to provide the greatest amount of flow for the least cost. The demonstration of the use of such a predictive computer model on data from the Roosevelt Hot Springs Known Geothermal Resource Area (KGRA) was the objective of this project.

In order to run the two-phase flow computer model, input data that defined characteristics of the well and the reservoir surrounding it were needed. For the Roosevelt Hot Springs KGRA some of this information was readily available, but temperature and pressures in the wellbore and especially at the production horizon as a function of flowrate were unknown. Under another contract with the Department of Energy, the Denver Research Institute had developed a logging tool to measure pressure and temperature in real time as a function of depth in flowing geothermal wells. The plan was then to use this equipment to conduct a series of tests of a particular well at various flowrates that would provide the data necessary to use the predictive computer model.

Flow tests of geothermal wells have been conducted previously by DRI, so that the logistics of arranging such a test were well understood. There are two areas of concern that must be addressed before the testing can be performed. One is to develop an agreement between the well owner and DRI that details liability coverage for property damage, particularly to the well, and personal injury. The coordination of the testing among the participants also becomes a significant task, because a minimum of three organizations (and often more) are involved: the owner, DRI, and the supplier of the seven-conductor wireline rig necessary to perform the logging. In the two series of well tests conducted as part of this project, as many as ten organizations were involved in testing, preparation of the site and wellhead, sampling of fluids, and support of the logging efforts.

In summary, the objectives of the project were as follows:

- to flow the geothermal well "Utah State" 14-2 at Roosevelt Hot Springs KGRA, Utah so that logs of pressure and temperature as a function of depth could be obtained;
- to collect samples of fluid (both liquids and gases) from the flowing well for analysis;
- to use the data acquired as input to a computer model which would in turn produce information indicating maximum flow rates as a function of casing schedules for the subject well.

The project was funded as part of the DOE/DGE "Industry Coupled" program, designed to promote exploration and development of geothermal energy. The Earth Science Laboratory of the University of Utah Research Institute is acting as coordinator for all information that will be obtained under this program. The data will be analyzed, and UURI will produce a report which presents the geothermal development technical feasibility for the target area.

The participation and cooperation of Thermal Power Company, operator of the geothermal well tested, and its partners in ownership, AMAX Exploration Company, and O'Brien Resources Company, must be commended. Certainly, without their interest and support this study would not have been possible. In addition, the contribution of a 7-conductor wireline rig and expert personnel by the U.S. Geological Survey, Water Resources Division, Borehole Geophysics Group, under the direction of Dr. W. Scott Keys proved to be invaluable.

This report has been prepared with the use of both SI (metric) and traditional (English) in the text portions; all data in tables and graphs are presented in English units only: the data was originally reduced to English units, and these units are still in common use by all major geothermal corporations in the U.S. Since this document is destined for use by those development companies, the English units have been retained.

II. FIELD TESTS

A. Test Plan

In order to perform computer modelling of the Roosevelt Hot Springs KGRA, data concerning downhole pressures and temperatures during flow were needed, as well as information on the composition and quantity of solids and gases dissolved in the geothermal brine. Since this information was not available from other sources, plans were made to flow the well "Utah State" 14-2, operated by Thermal Power Company, for several days during which the necessary data would be obtained.

The geothermal well "Utah State" #14-2 is located in the Roosevelt Hot Springs KGRA in southwestern Utah, and is owned jointly by Thermal Power Company, AMAX Exploration Company and O'Brien Resources, with Thermal Power acting as the operating partner. The well is approximately 6100 ft (1860 m) deep, and is cased with K-55 grade, 9 5/8 inch (24.4 cm) outside diameter casing to a depth of 1806 ft (551 m). Below this level to total depth, the well is open hole, drilled with an 8 1/2 inch (22 cm) diameter bit. It is suspected that there are several zones of flow in the well, but for the purposes of these tests it was assumed that the entire flow into the wellbore occurred between the 2900 ft (884 m) to 3000 ft (915 m) level. There is strong evidence in lithologic and other logs that a majority of the flow does indeed enter the wellbore at this level, so that the above assumption is reasonable.

A test plan to acquire the necessary data was prepared and the scheduling of participation by the organizations involved was completed. After an initial attempt to arrange a test in 1977 failed, agreement was reached on test dates in May of 1978. The tests planned for that time period included four elements:

- o shut-in (before flow) logs of wellbore temperature, caliper (inside diameter) and spectral gamma radiation level;

- o measurement of wellbore pressure and temperature as a function of depth under two-phase flow conditions;

- o surface sampling of brines and gases during flow;

- o downhole sampling of brine after shut-in of well following flow tests.

The surface sampling of geothermal fluids was accomplished by several groups: one from Battelle-Pacific Northwest Labs and one from The Earth Science Lab at the University of Utah Research Institute. Samples of both liquids and gases near the wellhead were taken, and analyzed for chemical content.

All logging functions were performed by the U. S. Geological Survey, Water Resources Division, Borehole Geophysics Group, under the direction of Dr. W. Scott Keys. This group operates a seven-conductor wireline rig that is equipped for high temperature geothermal work, including 15,000 feet of cable and a most complete electronics and data acquisition system. The planned sequence was to run several geophysical logs for later interpretation by USGS, then log the well with the DRI pressure/temperature probe under flow conditions, followed by the downhole sampling after completion of flow. The downhole sampler was a unit supplied and run by personnel of Los Alamos Scientific Labs. The unit had been developed at LASL, and had proved to be very useful in their Hot Dry Rock Program .

Other support needed for the May 1978 test included a mast truck to hold the upper logging sheave above the riser assembly, construction work on the brine holding pond, and some welding and fabrication of the flow pipeline. In addition, it was necessary to rent a valve and associate hardware to mount the riser assembly on the wellhead. The valve permitted isolation of the logging tool from the flowing well for maintenance and repair purposes.

A key element in the progression of events leading to the field test was the signing by the major parties involved of an Agreement detailing respective responsibilities in terms of personal and property liability and the disposition of data obtained during the tests. The Agreement was an institutional barrier that was hurdled through the work and ability to compromise of all participating organizations. Its execution served to show that institutional and technical objectives can be complementary to each other.

The May 1978 tests were disappointing in that only pressure data was recovered during the two phase flow logging. Due to a degradation of the conductor electrical insulation as a function of temperature leakage between conductor pairs measured as low as 200 ohms. This caused an effective short across the temperature sensor, and further, prevented operation of the LASL downhole sampler. Surface samples and USGS logs run under no-flow conditions were successfully operated.

Because of the problems encountered with logging cable performance noted above, disucssions concerning a repeat of the flow tests were begun in summer 1978. The USGS ordered and had installed by October, 1978, a new, high temperature-resistant seven conductor cable built by Vector Cable Company. It was felt that with this new cable, pressure and temperature data could be successfully recovered under flow conditions. Testing was not conducted over the winter months due to the severity of weather known to occur at the test site, so that the retest effort was scheduled for May, 1979.

The scope of testing planned for the second attempt in May, 1979, was limited to logs to be made by USGS and DRI. Encouraged by information developed from the logs taken during the 1978 test period, USGS returned and conducted additional logging for three days. Unfortunately, USGS equipment performance problems were encountered, and a minimum amount of new data was obtained. However, the DRI tool was run under flow conditions and successful logs were obtained at three flowrates. Some temperature-related problems were experienced with the DRI equipment, so that two additional logs were interrupted with failures.

The data obtained during the two tests of the well "Utah State" 14-2 provided all the needed information to perform the proposed analysis. Important data gathered included depth logs of pressures and temperatures at several flowrates, as well as an analysis of the chemical content of the fluid. Flowrates were measured by the James method, which uses an orifice pressure drop, upstream pressure and discharge lip pressure in an iterative scheme to calculate total mass flow.

B. Equipment

The probe used to acquire pressure and temperature data was one designed and fabricated by DRI to run both sensors simultaneously with a real-time readout. Temperature measurements are made with a platinum element resistance temperature device (RTD) which was operated in a four-wire configuration. The pressure transducers used in the probe employ a helical Bourdon tube made of Inconel to operate a potentiometer. The pressure transducer is also operated in a four-wire configuration. The original DRI probe was used to obtain most of the data during the Utah tests. In addition, an improved version that also incorporates a flow meter and a sensor to detect the phase (steam or liquid water) of the fluid moving past the probe was run in the 1979 tests.

A four-wire measurement technique is used to negate the effects of lead wire resistance and changes in lead wire resistance as a function temperature. The sensors are operated on a seven conductor logging cable, which is typically 15000 ft (4.6 km) in length. Because of this extreme length, the resistance of the lead wires is on the order of the sensor resistance (150 to 200 ohms per conductor, or 300 to 400 ohms when measured across terminals in the logging truck). By putting a constant current across the sensors and monitoring the potential drop on each with additional pairs of leads, the relatively large resistances in the cable can be bypassed.

The RTD has an ice point ($0^{o}C$) resistance value of 100 ohms, which becomes about 200 ohms at $500^{o}F$ ($260^{o}C$). When run with a constant current of one milliamp, the potential drop across the RTD ranges from 100 to 200 millivolts. Calculations have shown that a constant current on the order of one milliamp to be optimum. Larger values can lead to significant self heating of the element and smaller values reduce the signal level to where signal to noise ratio becomes too low to allow accurate interpretation.

The RTD's used in both DRI probes are supplied with a factory calibration table. The units are placed in eutectic mixtures maintained at five different known temperatures. The output of the RTD at those known temperatures is then used to calculate the coefficients for a quadratic equation which describes the relationship between resistance and temperature for the serially number RTD under test. The calibration table then is printed by computer, giving resistance values for every $2.5^{o}F$ ($1.4^{o}C$). The manufacturer guarantees that these units yield results within $\pm$ $0.1^{o}C$ of the actual temperature, when values between the numbers on the cal table are linearly interpolated.

The pressure transducer potentiometer is a 0-1000 ohm unit wound with 330 turns. The transducer range is 0 to 2000 psia (0 to 13.8 MPa), so that the resolution of the sensor is 6 psi/turn (41 kPa/turn) of the pot. Wiring of the constant current log of the pressure transducer is in series with the RTD, so that the same level of current is present. The signal output is then 0 to 1000 millivolts, nominally. The pressure transducer is calibrated before each field test in the instrumentation lab of the Laboratories for Applied Mechanics with a dead weight tester that is certified to have errors of less than 1/3 of 1%. Through use of this calibration technique, it is felt that the manufacturer's claim of accuracy within 1% of actual value is maintained.

The readout system that is used for the DRI probe provides power as well. A digital voltmeter (DVM) with an optional "true" four wire capability is used to provide the constant current, as well as the potential drop measurement across one of the sensors. A second DVM operated as a straight voltmeter provides the readout of the potential drop across the other transducer (Figure 1). The "true" four wire capability is important, because the constant current circuitry must have a broad dynamic range. For the case of the DRI probe, the resistance of the conductors carrying the constant current to the transducer element is on the order of the value of the resistance of element itself. Further, the resistance in the plus and minus current leads is unbalanced, because the resistance of the other sensor element is added to one leg. The end result is that the constant current circuit for the case presented must have a voltage four to five times larger than the voltage necessary to make the four wire measurement of a single sensor without the 5km cable leads.

A CIMRON model DMM-52 DVM, which meets the above operational criteria is used in the DRI system to supply the constant current and provide one of the readouts. The second readout is provided by a DANA DVM owned by USGS. Both units have analog outputs which are connected to strip chart recorders. These recorders produce the permanent data records which are then reduced by reference to the calibration curves monitored earlier. The strip chart recorders are slaved to the footage counter on the logging cable, so that all data is recorded as a function of depth, with an option to also take data on a time drive basis. The recorders are equipped with offset pots and wide band span adjustments, so that a wide variation in input signal level can be accommodated.

Several features of the mechanical layout used by DRI in geothermal well logging should be noted here. The wellhead was modified by the

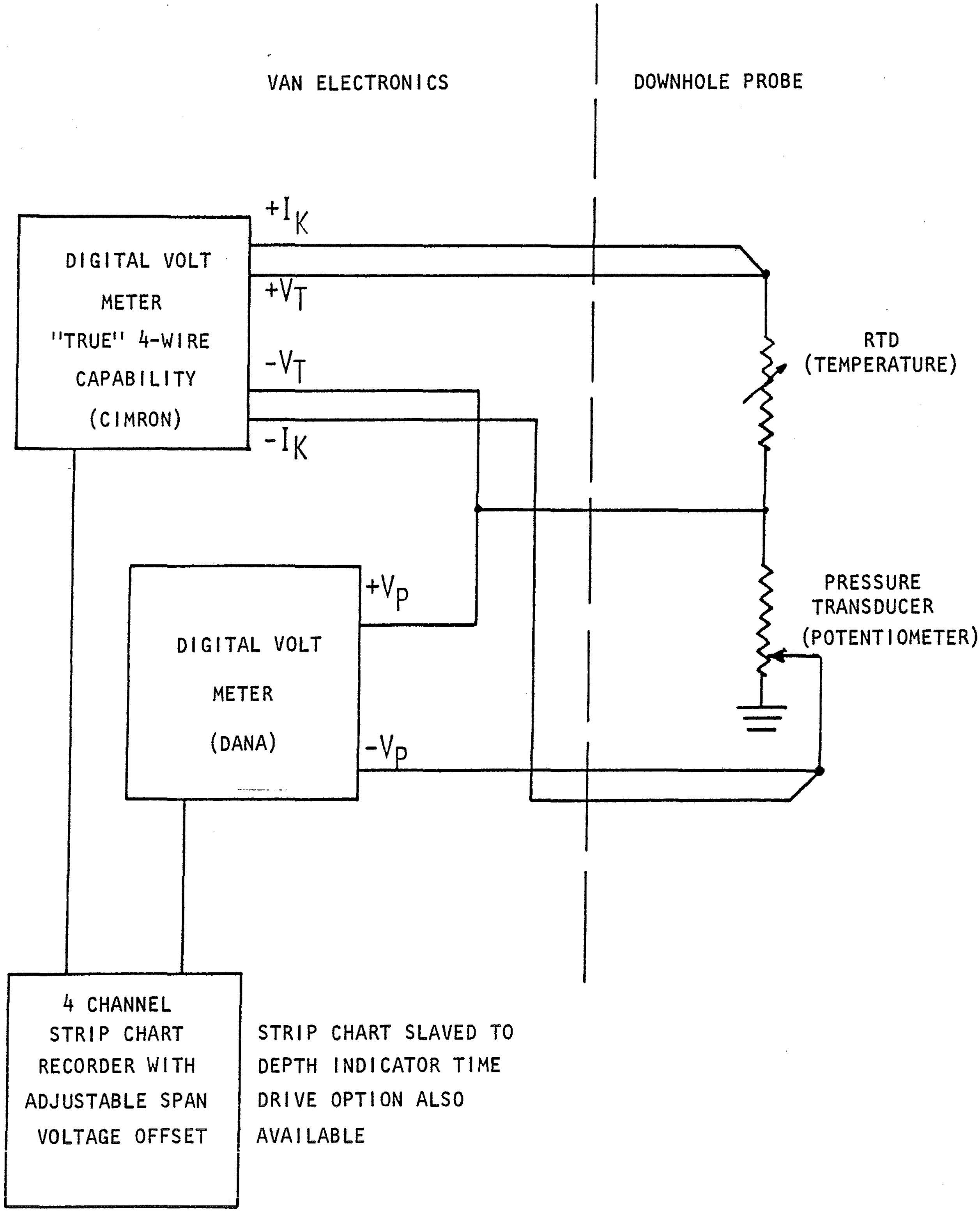

FIGURE 1. DRI PROBE AND DATA ACQUISITION SCHEMATIC.

addition of a large diameter isolation valve (6 inch or greater) to which the riser assembly was mounted. The riser consisted of 2 lengths of 6 inch (15 cm) diameter pipe, each 8 1/2 feet (2.6 m) long joined by hammer unions with a pressure control device at the top, and a short 6 inch (15cm) diameter stub at the bottom, which was threaded into a flange mated to the isolation valve. A 3/4 inch (1.9 cm) valve is welded to the riser pipe near the bottom to provide pressure relief of the system after closure of the isolation valve.

The tool was mated to the cable with a seven conductor cable head connector designed and built by Gearhart-Owens. Directly above the cable head, three lead sinker bars were installed, each of which weighed about 50 lb. (16 kg), for a total of 150 lb. (48 kg). The tool string was thus about 20 ft (6 meters) long, which is why the long riser assembly was needed. Centralizers were attached to the tool string in two places, to keep the instrumentation centered in the wellbore. Sinker bar was employed to assure that the tool would not be thrown from the well during flow. In particular, slug flow in the two-phase region can cause high velocity liquid slugs trapped between accelerating gas (steam) bubbles to impact on the tool.

The tool itself is designed to present a minimum cross section (2 in. or 5cm diameter) to the flow so as to reduce the possibility of lifting the tool with the two-phase flow. The pressure port is located on the side of the tool to measure static pressure, while the RTD is protected by a cage arrangement which prevents damage to the sensor while permitting ventilation of the RTD stem by fluid moving past the probe.

The US Geological Survey, Water Resources Division, Borehole Geophysics Group operated the wireline rig used in the tests. This unit carries 15000 ft (4.6 km) of seven conductor logging cable on a hydraulically operated winch. AC power is provided by two gasoline generators, so that the logging unit is self contained. The logging van is equipped with an extensive array of electronic instrumentation which permits operation of the DRI probe and permanent recording of the data displayed.

During the May, 1979 tests, a cable cooler was installed to cool the high performance cable before it crossed the upper sheave. The cooler consisted of a 2 inch (5 cm) pipe about 15 ft (4.6 m) long into which the cable passed after exiting the pressure control device atop the riser assembly. The cooler was mounted vertically above the riser, and was filled with water that was circulated by a pump. The cable manufacturer had recommended cooling the cable before it passed over the top sheave to prevent extrusion through the armor strands of the conductor insulation, which softens at high temperature. The system appeared to work quite well since the cable was cooled to ambient temperature by the time it reached ground level.

Operational problems occurred during both tests, as is the norm in field testing, particularly when equipment is subjected to the severe conditions of a high temperature geothermal well. Several materials failures in the DRI tools were noted, particularly with "high temperature-resistant" silicones. USGS also experienced recurring problems with the cable head termination. The plastic molded connector plugs used in the cable head developed pin to pin electrical leaks on the order of 20 to 30 kohms after exposure to the fluid of several hours. In addition, no grease or fluid tested was retained in the cablehead for more than one day's operation, and the flexible rubber boots used as a protective sleeve on the high temperature solder joints showed a tendency to depolymerize and disintegrate. Because of the above described failures, considerable time was spent in repairs and remakes of the cablehead.

C. Test Data

The information gathered during the May 1978 and May 1979 flow tests of "Utah State" 14-2 is presented in Figures 2 through 8 and tablated in Appendix A. As noted earlier, the 1978 testing acquired pressure data only, while both pressure and temperature information was recovered during the 1979 tests.

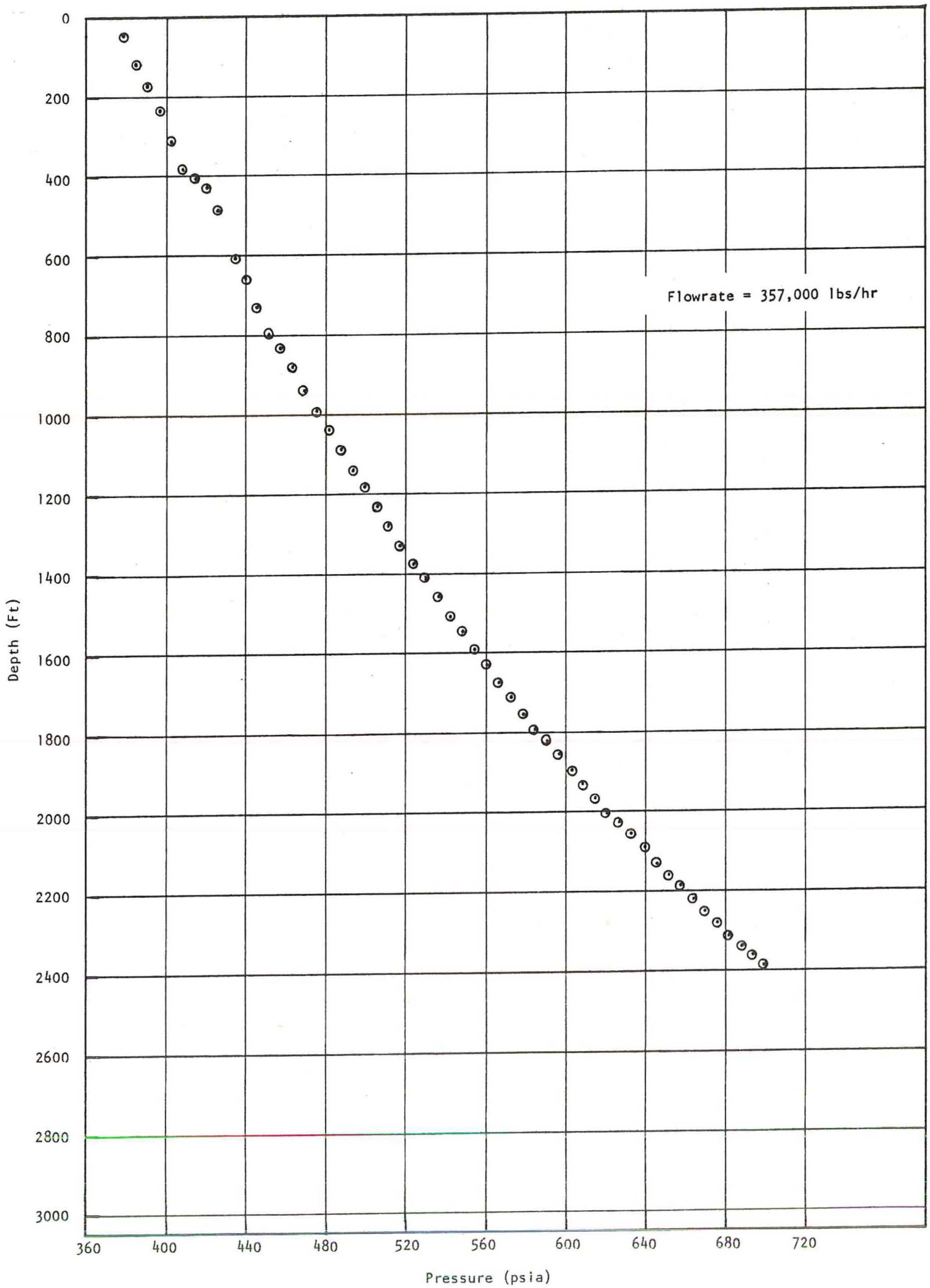

Figure 2. DATA FROM LOG #2, MAY 1978 TESTS

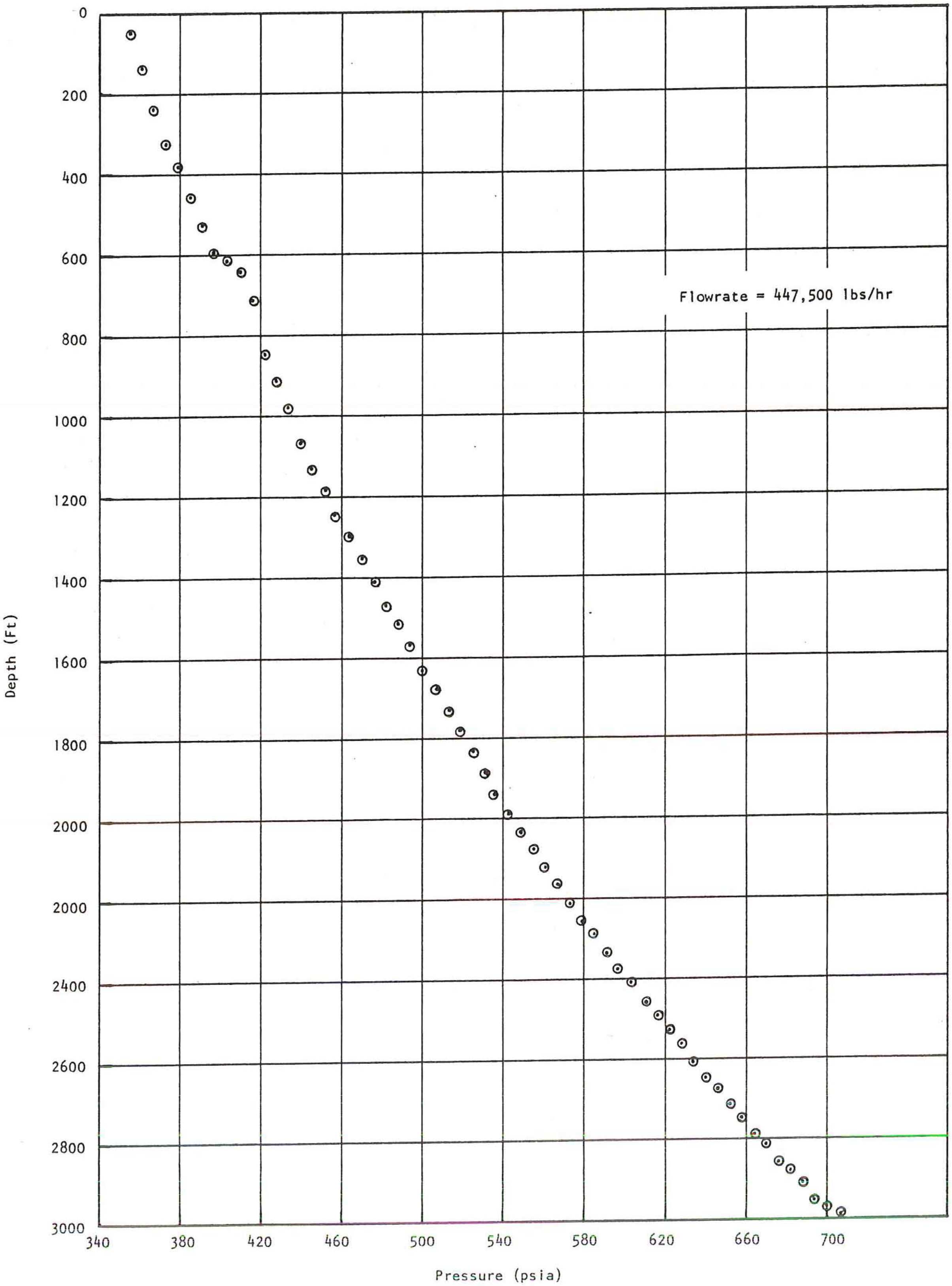

Figure 3. DATA FROM LOG #3, MAY 1978 TESTS

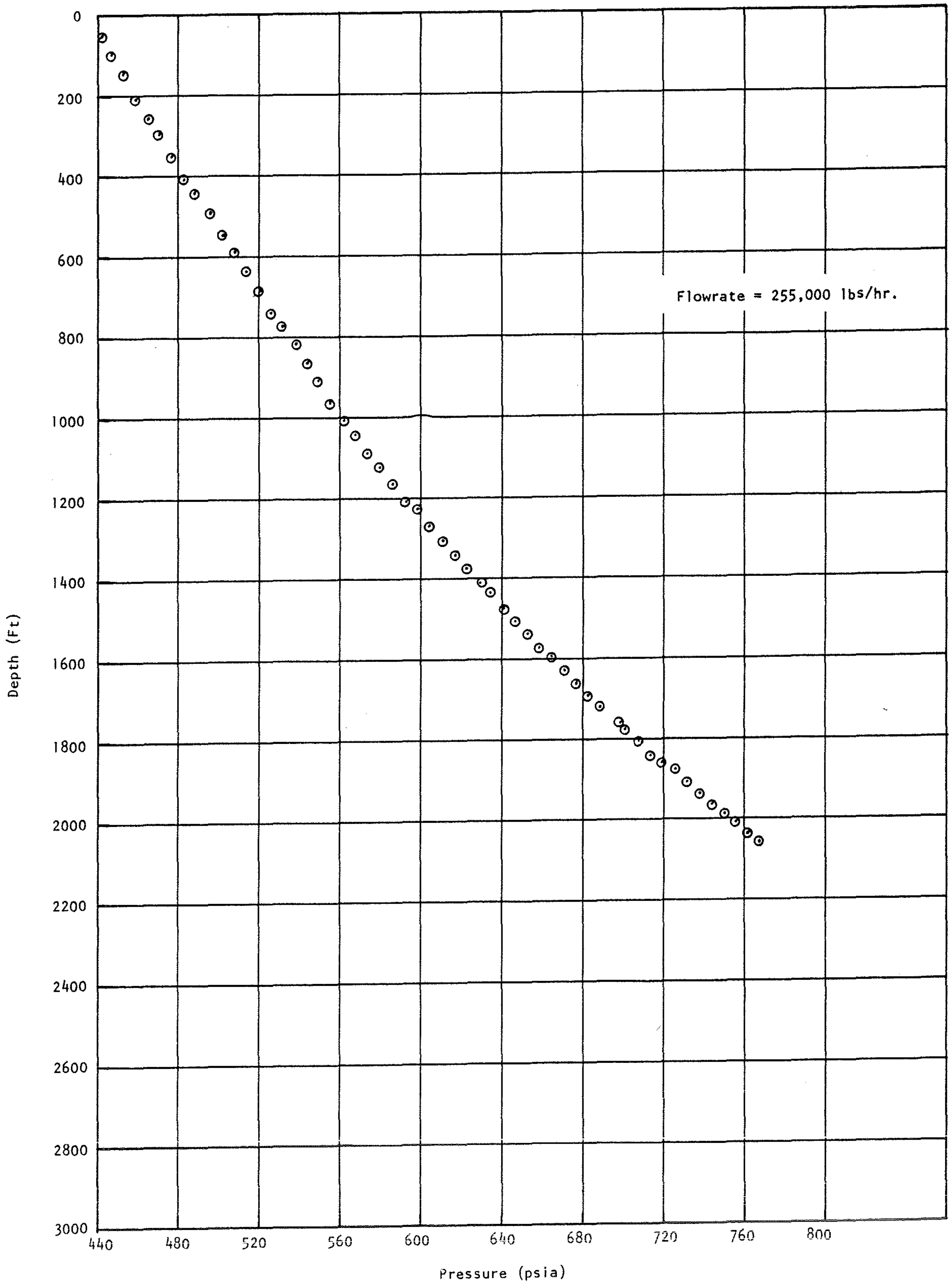

Figure 4. DATA FROM LOG #5, MAY 1978 TESTS

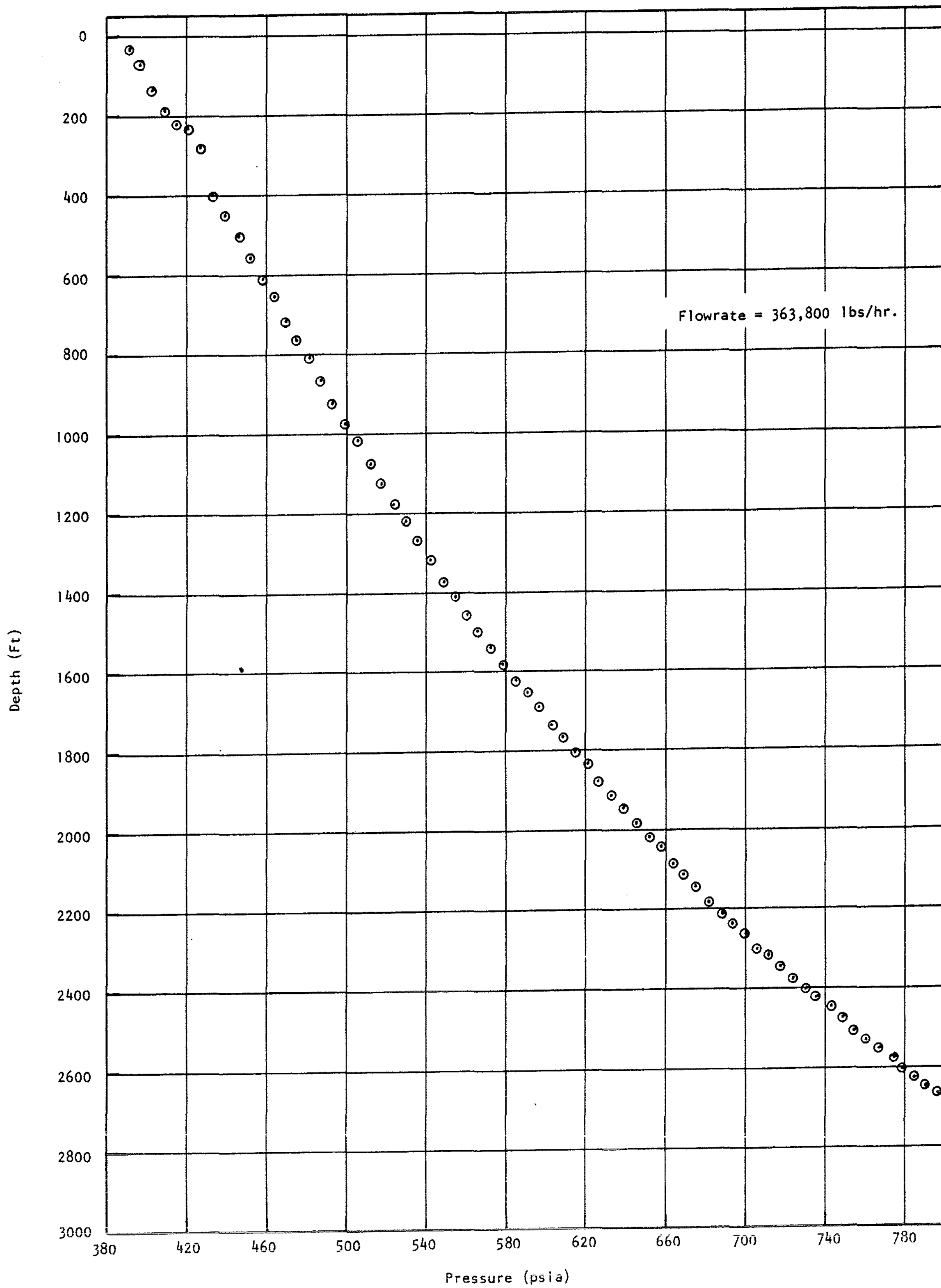

Figure 5. DATA FROM LOG #6, MAY 1978 TESTS

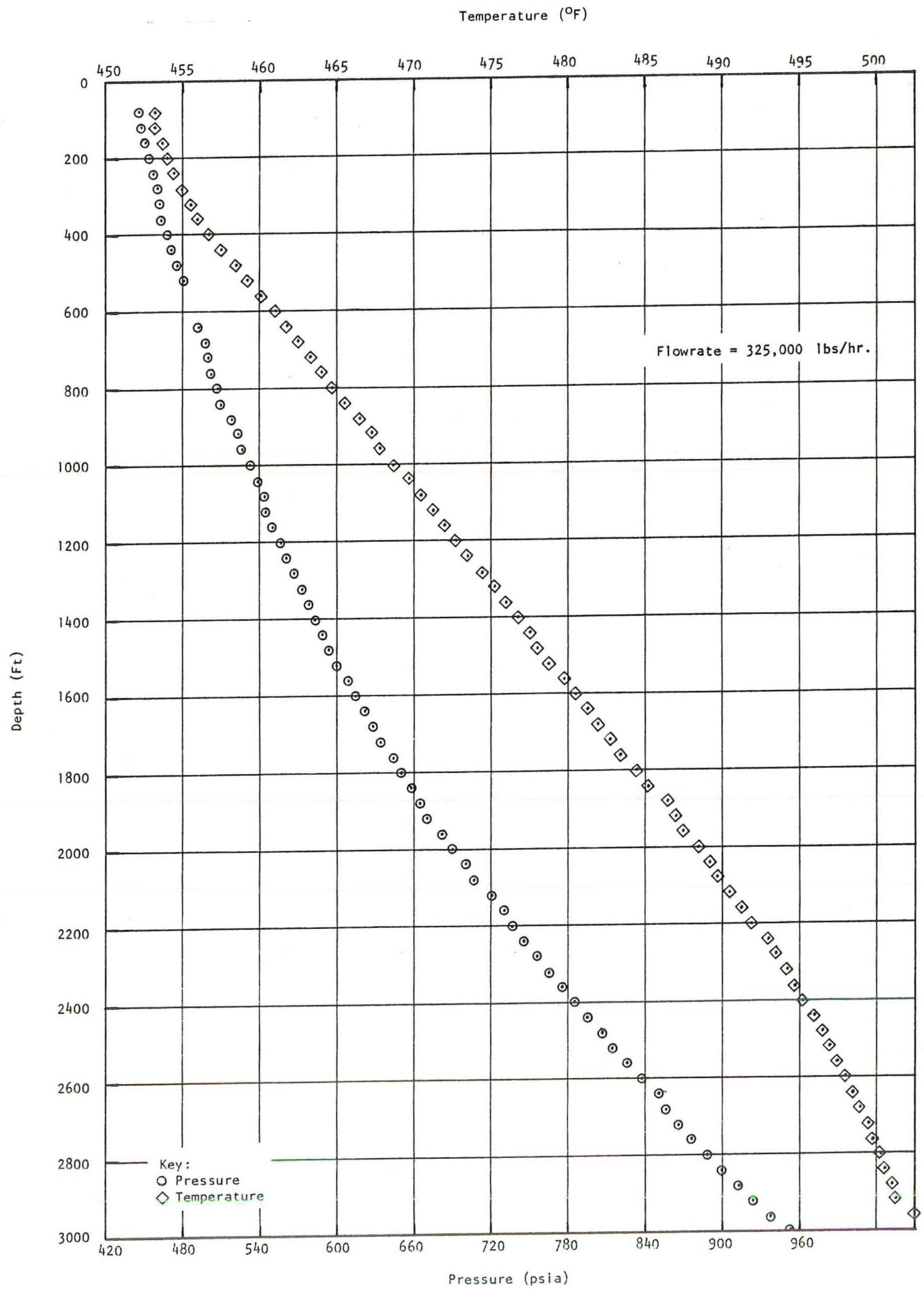

Figure 6. DATA FROM LOG #2, MAY 1979 TESTS

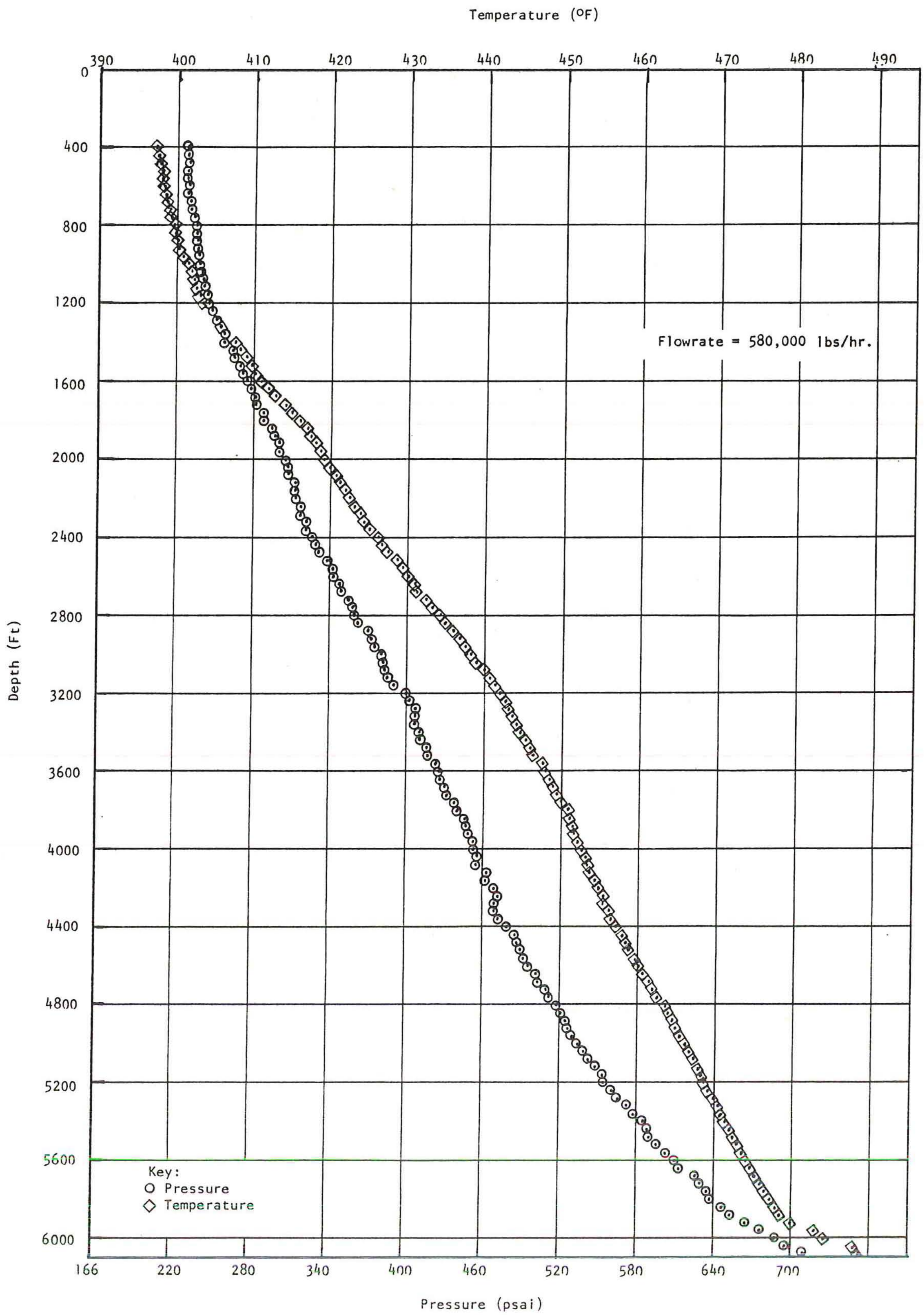

Figure 7. DATA FROM LOG #4, MAY 1979 TESTS

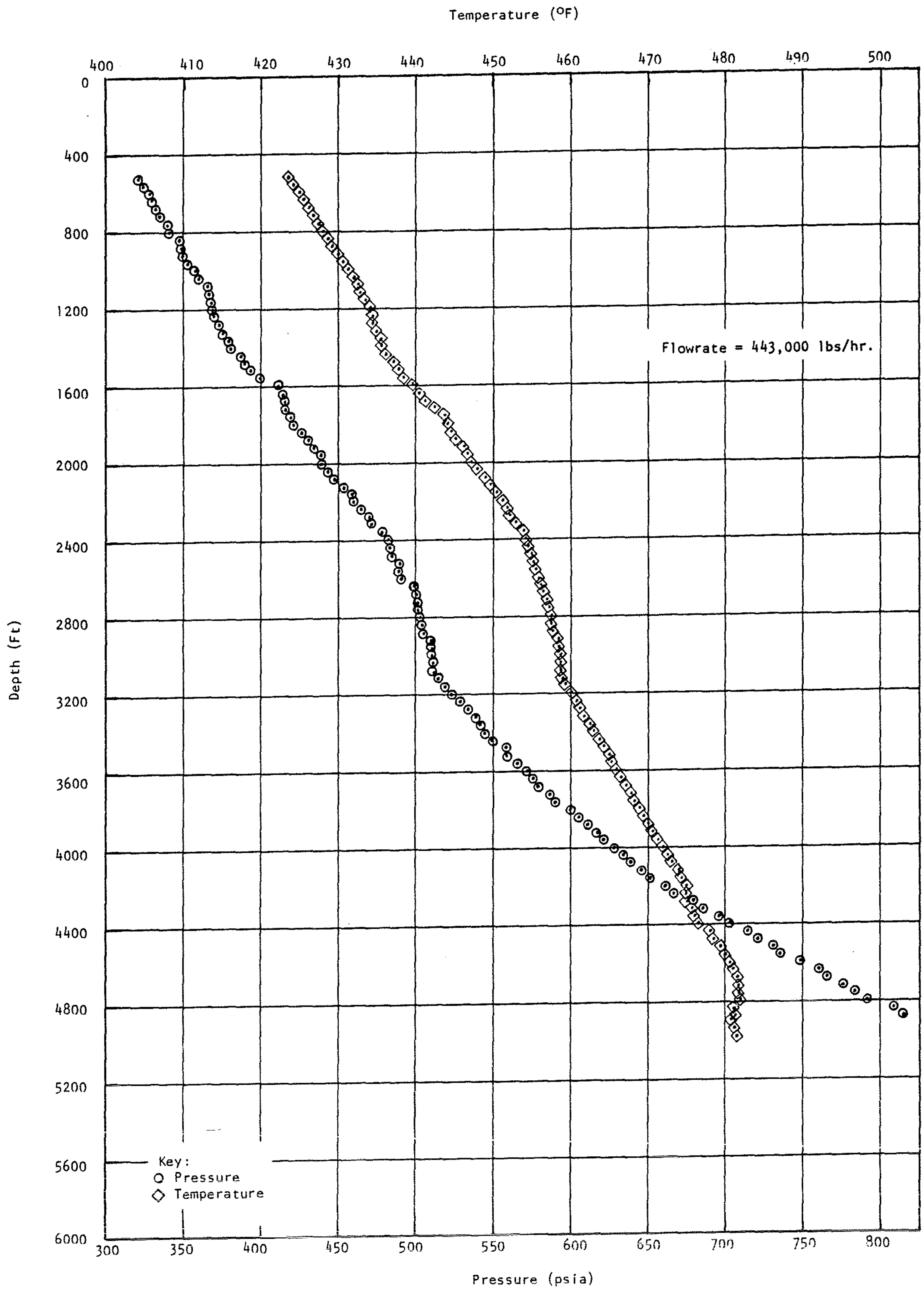

Figure 8. DATA FROM LOG #5, MAY 1979 TESTS

III. DATA REDUCTION AND ANALYSIS

A. Impact of Two-Phase Flow

Two-Phase flow is initiated in a flowing well where the static pressure of the fluid in the wellbore drops to the saturation pressure for the temperature of the flowing fluid. If the pressure never drops below the saturation value, the well is in single phase flow throughout the length of the wellbore. Two phase flow influences both the temperature and pressure drops in the fluid during its rise to the surface. The pressure drop and temperature change are related through the saturation pressure/temperature curve for water. Certainly, dissolved gases and solids can modify the specific values of points on the curve, but the principle of a one to one correspondence between temperature and pressure in a two-phase mixture remains valid.

The pressure drop in a two phase mixture is the sum of three components: a hydrostatic head, a friction pressure drop and an acceleration pressure drop. This contrasts with only two components in a single phase flow, the hydrostatic head and friction pressure drop. A quick calculation shows that for typical geothermal fluid densities and flow velocities, the hydrostatic head accounts for about 97-99% of the total pressure drop in single phase flow. The distribution among the three components in a two-phase flow varies as a function of the relative amounts of liquid and gas.

This becomes logical when the difference in density between liquid and gas (steam) phases of water is considered. When there is a relatively small amount of gas, the hydrostatic head term remains dominant, although not to the extent of single phase flow. As the gas phase becomes an increasingly larger fraction of the total flow, the pressure drop distribution among the three mechanisms begins to shift for several reasons. The hydrostatic head drops significantly, as the less dense gas phase displaces water in the column. At the same time friction is increased because the gas phase must move at a higher velocity to maintain continuity of mass in a constant area cross section pipe. Friction occurs between the phases, as well as between each phase and the pipe wall. Finally, the energy expended in accelerating the gas phase to the above noted higher velocity relative to the liquid is manifested as a pressure drop.

As the volume (and mass) fraction of gas increases, there occurs a succession of flow regimes that can be categorized by a description of which fluid phase is continuous and which is dispersed. When two-phase flow is just beginning, many small bubbles tend to nucleate and are carried along in a continuous liquid phase. The bubbles grow and coalese until they reach a size on the order of the pipe diameter, at which point slug flow is entered, where continuous gas and continuous liquid phases alternate in the pipe. These large gas bubbles then grow to a size where they break through the liquid slugs, and the churn flow regime is created. Here neither phase is continuous in any pattern, and a random flow is observed, as the name implies.

The phase change proceeds, driven by the pressure drop as the flow rises up the wellbore. Enough gas has now evolved that it forms a continuous column rising up the center of the well, with a much slower-moving liquid annulus clinging to the wall in the annular flow regime. Finally, the gas reaches such a high velocity that the liquid annulus is ripped from the wall by friction forces, and mist flow is established, with a continouous gas phase and dispersed droplet liquid phase that is the inverse condition from the initial bubble flow regime.

It can now be seen that an indication of two-phase flow and the point of transition to that flow should be noticeable in the pressure and temperature gradients measured in a flowing geothermal well. The pressure gradient will change as the relative contributions vary, as described above. To appreciate the magnitude of the pressure gradient variation, it should be noted that two-phase flow pressure gradients as small as 10% of single phase values can exist in certain flow regimes. In addition, the temperature changes to follow the temperature/pressure saturation curve. This heat exchange is easily accounted for by the trade of sensible heat in the fluid for latent heat of vaporization, causing the production of the gas phase.

For the case of pure water, the development of two phase flow is straight forward, as described above. The addition of dissolved solids and gases provides complication in that the interaction of the chemical species is a function of the changing temperature and pressure, causing a constant shift in equilibrium conditions. Dissolved solids impact the flow in two ways: First, the dissolved solids can change the density of the fluid and cause a slight shift in enthalpy content and boiling point; second, as some of the flowing liquid is flashed to steam, the dissolved solids concentration may exceed the saturation level, causing nucleation and formation of scale on the wellbore.

Consideration of dissolved gases adds another level of complexity to the chemical and physical processes. In high enough concentrations, dissolved gases will begin to nucleate and form bubbles at pressures higher than the saturation value for pure water. The nucleating gas then provides a gas phase partial pressure sufficient to cause the creation of a gas phase of the liquid water (steam production). In other words, when the dissolved gas concentration is sufficiently high, two phase flow can be initiated at pressures well above the saturation value for pure water. In such a case, the gas phase will always be composed of a mixture of steam and the one or more gases present, because the nucleating gas and steam are evolved simultaneously.

There is an additional important impact of dissolved gas in a two-phase flow system. Certain species of dissolved gas (carbon dioxide is the most common) act as a buffer when in solution, so that as the gas begins to nucleate and the concentration in the solution decreases, the pH of the fluid changes. When dissolved solids are present in the fluid, this pH change can cause a significant shift in the chemical equilibrium, forcing a supersaturated condition and consequent formation of scale. Gas content on the order of 1%, a level commonly found in geothermal wells, is sufficient to cause the effects noted above.

This discussion can be summarized by stating that two phase flow is influenced by a number of parameters, which are noted below:

o dissolved gases and solids (as described above);

- o temperature-saturation pressure is a monotonically increasing function of increasing temperature, up to the critical conditions ($705^{o}F$ or $374^{o}C$);

- o downhole production zone pressure - the value of production pressure will dictate what proportion (if any) of the wellbore will be in two-phase flow;

- o casing schedule-diameter of the wellbore will determine liquid and gas velocities, which are influential in the holdup and friction pressure drop contributions to the total two phase pressure drop;

- o flowrate - a second parameter that governs velocity is the flowrate, so that its impact is also felt in the friction term of the pressure drop. In addition, the production zone pressure decreases with increasing flowrate (so-called "drawdown") which also changes the available pressure drop in the wellbore and thus the length of wellbore in two-phase flow.

For the KGRA and well under study, the temperature and solution chemistry are fixed; the subject of investigation, therefore, will be the change in maximum flowrate as functions of casing schedule and productivity index (a measure of production zone pressure change due to flow in the well).

There is an additional process that may exert an influence on the two-phase flow, that of heat transfer from the flowing fluid to the surrounding rock strata. In the single phase flow region, this heat transfer is the mechanism that causes a drop in fluid temperature, and thus lowers the (saturation) pressure at which two-phase flow is initiated. In the two-phase flow zone, the loss of sensible heat to the wellbore will result in less sensible heat being available to convert to latent heat in the flash process, and thus a smaller quantity of steam will be evolved in the two-phase flow. That is to say, the wellhead fluid will have less enthalpy on a per-unit mass basis. Sample calculations for typical geothermal conditions have shown heat transfer effects to be minimal, yielding enthalpy losses of less than 1%. Therefore, the flows in this analysis will be considered to be adiabatic - having neither heat loss nor gain as the fluid moves up the wellbore.

B. Reduction of Field Test Data

The raw data from the field tests was recorded on rolled paper with a strip chart recorder. The recorder featured variable span and voltage suppression controls so that the recorder scale could be expanded to the range of interest. For both tests, the strip chart units were set to display both temperature and pressure on two traces each. One trace for each parameter was set so that the full range of interest spanned the chart paper. A second trace was then set to be an expanded scale, with a greater "gain" to allow more precise determination of resistance values and also to permit easier observation of small perturbations in the measured quantities.

During the 1978 tests, severe problems with cable performance (noted previously) were encountered, and the resistance data obtained was meaningless as an indication of parameter values. However, because of the design of the pressure transducer, pressure data was successfully recovered for the tests. The unit employs a helical Bourdon Tube to operate a 1000 ohm potentiometer. There are 330 turns in the pot, so that as the wiper moves from one turn to the next, a three ohm jump in resistance is seen on the output record. These jumps are clearly visible on the strip chart, in spite of a general decline in the resistance value during the period that the wiper remains in contact with a particular turn of the pot. The wiper will remain in contact until sufficient additional pressure to move it to the next turn is encountered. This differential pressure has been measured in the laboratory to range from 4 to 7 psi (28 to 48 KPa). As the probe is lowered into the flowing well, the pressure on the Bourdon tube element increases until the above-specified differential is reached, at which time the wiper advances to the next turn.

Figure 9 is a sample section of the data chart, showing the (apparent) negative temperature gradient and several wiper steps of three ohms each

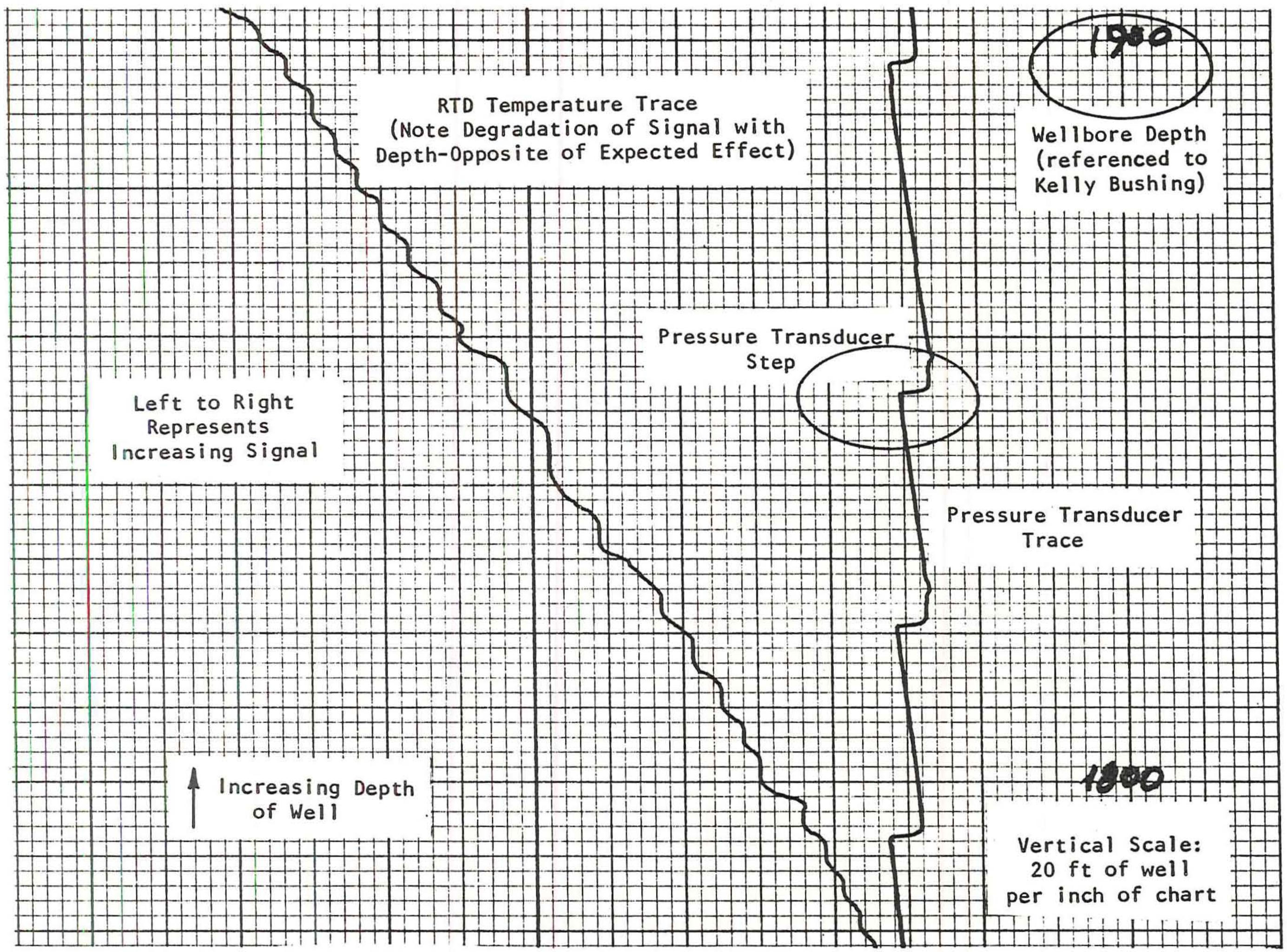

Figure 9. Typical Strip Chart Data, May 1978 Tests.

(although due to parallel resistance effects, each step measures at about two ohms). The pressure reading can be found by reference to the value with the probe at the wellhead, which, in turn, is determined from a calibration curve, since there is no cable immersed in the flowing fluid. Each step is then considered to be 2000 psi/330 turns = 6.06 pounds per square inch (41.8 KPa). The pressure reading at any step can now be determined by adding the product of the number of steps and the per-step increase to the wellhead reference pressure. The data obtained during the May 1978 tests was reduced as described above, and is included in this report in section II.

The USGS seven conductor logging cable was replaced in October 1978 with a new, high temperature-resistant cable manufactured by Vector Cable Company, and designed to operate at a maximum temperature of 550°F (288°C). Additional well tests were then run in May, 1979 with this new cable. The operation of the DRI probe was much improved; figure 10 shows a typical section of the strip chart record obtained in the 1979 tests.

Prior to field testing, all the pressure transducers were calibrated in the laboratory at temperature using a dead weight tester with maximum error of 1/3 of 1%. Calibration curves of sensor output versus pressure at several temperatures of interest were generated with the calibration data. New RTD temperature probes were purchased in January 1979, which were factory calibrated, and which included a calibration table. The calibration on these units was factory-certified to be within $\pm$ 0.1°C of the actual temperature.

The method of data reduction used to develop the tables of results shown earlier can now be stated. Displacement of traces from a baseline on the strip chart for pressure and temperature was measured and recorded on a data reduction sheet. An appropriate scale factor, taken from the strip chart calibration and values recorded in the log, was multiplied by the displacement recorded. This product was then added to the voltage value of the baseline, and the sum recorded as the transducers electrical output level. By reference to the calibration curves, these voltage levels were converted to engineering units. Linear interpolation was employed where necessary on the data points, which were

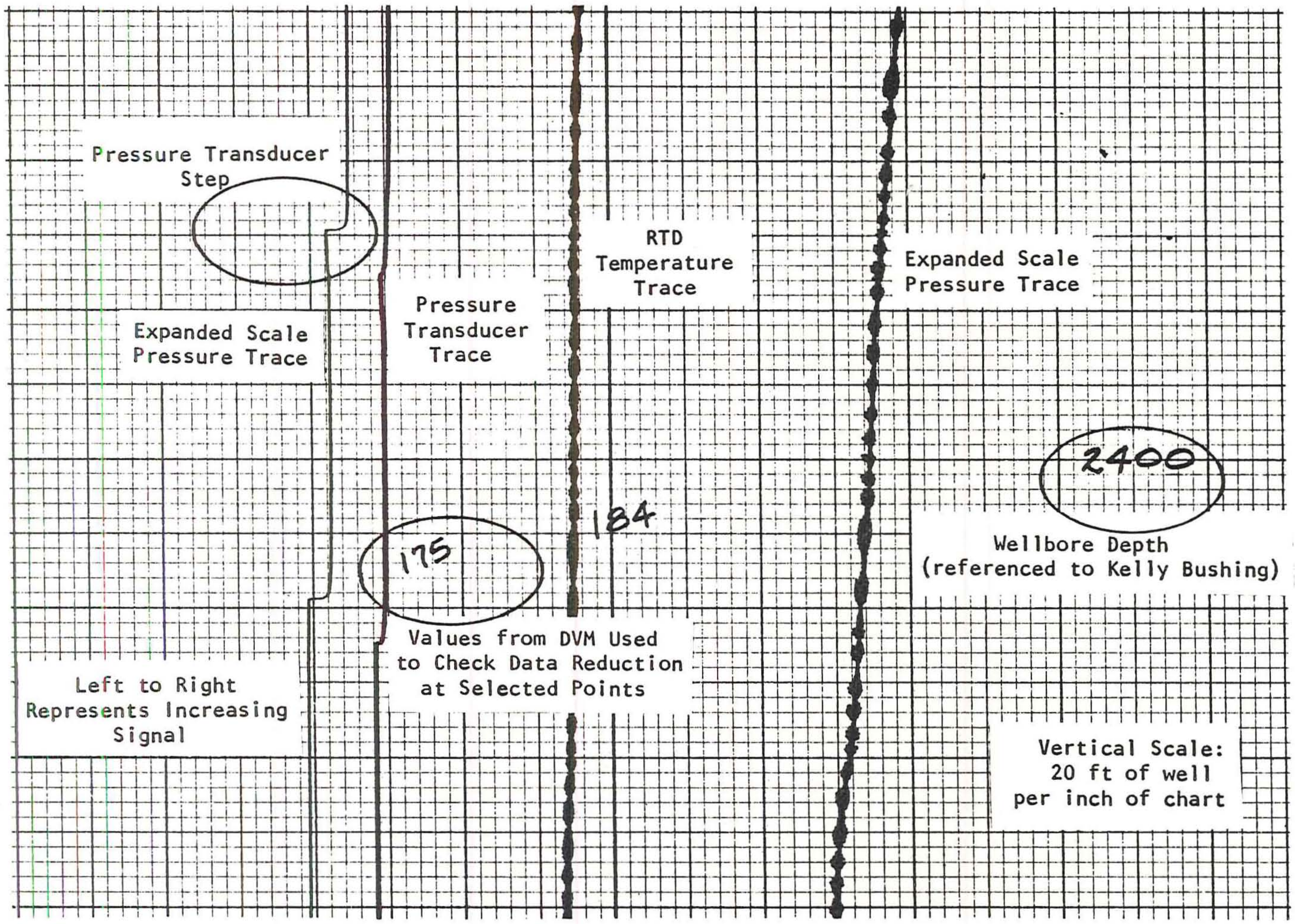

Figure 10. Typical Strip Chart Data, May 1979 Tests.

taken every 40 feet (12 m). Because of the high temperatures and consequent considerable length of two phase flow in this well, the above data spacing was deemed to be quite adequate.

C. Preliminary Analysis of Field Test Data

After reduction to tables and graphic form, the 1978 data was examined to make an assessment of its validity. The technique of orthogonal polynomials was used to determine the optimal degree of least squares polynomial to which to curve-fit the data. The results indicated that a least-squares quadratic equation would be adequate. The data from all the logs was then curve-fitted, yielding correlation coefficients from 0.985 to over 0.999. The excellent fit confirmed the self-consistency of the data. Although there is no known direct correlation of two-phase pressure drop to some quadratic equation it can be expected that the phenomenon may be represented by a continuously differentiable ("smooth") curve, thus the outstanding fit certainly strengthened the level of confidence that was placed in the data.

However, further examination of the '78 data presented an interesting anomaly. At pressures greater than the saturation level for the known temperature in the well, the pressure gradient was considerably less than that of a single-phase flow. That is, the gradient appeared to be smaller than the hydrostatic gradient computed for an all-liquid flow. Of course the saturation pressure used in making the above comparison was the value for pure water. The logical conclusion, therefore, was that dissolved gases present in the well were causing an increase in the saturation pressure, and that a much greater length of wellbore was in two-phase flow than had been previously expected.

Several calculations were then made. Based on the assumption that the hydrostatic term in the two-phase pressure drop equation was dominant, the amount of carbon dioxide required to cause the observed depression in pressure gradient was computed to be less than one half of one percent of the mass flow, a level not uncommon in geothermal systems. Also, the saturation level of carbon dioxide in brines of the approximate temperature of the test well was calculated, and plotted as a function of pressure. At the measured shut-in reservoir pressure, these figures indicated that the saturation level of CO_2 in solution in the brine was over 2% by weight.

The suspected influence of CO_2 on the saturation vapor pressure (and consequently, the location of the flash horizon) was confirmed when a computer run was made with input conditions of measured pressure, temperature (from other sources), flowrate and casing schedule of the test well. Included in that computer run was a CO_2 level of one percent by weight in the flowing fluid. The result indicated that the CO_2 level introduced exhibited a considerable influence on the location of the flash horizon by causing an upward shift in the saturation pressure, from 702 psia (4.96MPa) to over 1000 psia (7 MPa), certainly a significant change. Quantitative information on the gas content measured during sampling of the well at the 1978 tests was not obtained until late in the program; however, the information showed a non-condensable gas content of about 0.8%, and that over 99% of the non-condensable gases were identified as CO_2.

The flowrates given for the test runs made during the 1978 and 1979 tests were conducted by use of the James method. This is an empirical technique for two-phase flow measurement developed by Mr. Russell James in the New Zealand geothermal fields. The method employs an iterative scheme to calculate the total mass flowrate, using inputs of pressure drop across an orifice, upstream pressure, and lip pressure at a discharge nozzle. During the '78 tests at Roosevelt Hot Springs, problems were encountered with the pressure drop measurement, so that an assumed enthalpy was used in the total mass flowrate calculation. Measurement of the upstream pressure became a problem in the '79 tests, and as a result, the flowrate values calculated for both years are assumed to have an accuracy of within $\pm$ 15% of the actual value.

Flowrate data is an important input to the calculation of the productivity index (PI) for the well and reservoir under investigation. The PI is a measure of the pressure drop that occurs at the production due to pressure losses generated by fluid motion through the reservoir to the wellbore. The defining equation for PI assumes that there is a linear relationship between the rate of mass flow and drawdown (pressure drop at the production horizon):

$$P_{pr} = P_o - {}^{Q}/J \tag{1}$$

where P_{pr} = pressure at the production horizon at flowrate Q

P_o = shut-in (no-flow) pressure at the production horizon

J = productivity index, in units of incremental flowrate per unit incremental pressure drop.

The importance of PI becomes evident when one objective of this study is brought into focus: to determine the maximum flowrate of the reservoir as a function of casing diameter. In this case, a minimum wellhead pressure is specified, a condition at which two-phase fluid will be supplied to the conversion system. As a result, the available pressure drop in the reservoir/wellbore system is established. The pressure drop is apportioned between the components of that system. With the reservoir pressure drop computed by use of the PI equations, and the wellbore fraction determined via the computer model. This cannot be done directly, so a methodology to extract the needed information has been developed, and will be explained later in this report.

For the data obtained during testing at Roosevelt Hot Springs, production horizon pressures were measured as well as flowrates, so that statistical techniques can be used to compute values for P_o and J in the PI equation. In doing so, several assumptions have been made that must be noted. The first and foremost assumption is that the production in "Utah State" 14-2 occurs in a highly fractured zone located between 2900 ft (884 m) and 3000 ft (914 m) in the wellbore. This assumption is based on a geologic log prepared by the Earth Sciences Lab at the University of Utah Research Institute, and also upon the data obtained during the tests run by DRI. Actually, it is suspected that geothermal brine may be produced from several zones in the wellbore, but it has been assumed that the zone noted above is the primary contributor.

Examination of the data obtained in the 1978 and 1979 tests reveals that pressures at the production horizon are not available for all logs. For some cases, projections have been made by curve fitting the available data to a quadratic equation, and then projecting a value for the production zone. A summary of this data is presented in Table 1.

Values for J, the productivity index, and P_o in the PI equation were calculated by use of a least squares linear fit of the test data noted in Table 1. The results of the procedures are also noted in the table. The calculated P_o was then used as the basis for the computation of pressure drop due to flow in the reservoir to the wellbore. This is a statistically determined value, and is greater than the measured shut-in pressure at the production horizon, as taken from logs run soon after completion of the well. Use of the PI approach permits a simple determination to be made of the drawdown at any flowrate.

The accuracy of passive temperature measurement systems (e.g., a platinum resistance thermometer down the hole, with a 4-wire connection to a read-out system on the surface) is limited because of signal transmission problems. Errors are caused by line and leakage resistances in the cable, and by leakage resistances in the cable head (the connection between the cable and the logging tool). An analysis of this problem, has been performed and the conclusions are (1) the best cables currently available are only marginally capable of achieving temperature measurements within $\pm$ 0.5^{o}C of actual values, and (2) cable head connections are even more of a problem. A summary of the analysis is contained in Appendix B.

TABLE 1

PRODUCTIVITY INDEX COMPUTATION "UTAH STATE" 14-2

	(log#)	$P_{downhole}$ (@2950') psia	Q lbs/hr.
'78 Data:	2	(868)	357,000
	3	694	454,000
	5	(975)	255,000
	6	882	369,000
'79 Data:	1	1001	284,000
	2	930	325,000
	3	(612)	505,000
	4	375	580,000
	5	511	443,000
Shut-in Data		1365	0

( ) indicates projected value at 2950'

Using all 10 data points: $P = 1428 - 1.698 \times 10^{-3}\ Q$

Coefficient of determination = -0.9257

$$J = 589\ \text{lb/hr/psi}$$

Note: Log #3, '79 data pressure at 2950 ft. is projected from data taken below 2950 ft., using a least squares quadratic fit. Logs #2 and #5 of '78 data are projected from data taken above 2950 ft. using a quadratic fit.

D. Approach to Computer Analysis

A computer model of two-phase flow in vertical wellbores is being developed by Coury and Associates, consulting chemical engineers under a subcontract to the Denver Research Institute. The modelling effort is part of an overall investigation of two-phase flow performed for DOE by a team headed by DRI. Arrangements were made to employ this model for the analysis of the data taken at "Utah State" 14-2 at the Roosevelt Hot Springs KGRA. Note should be made of the fact that the computer model has not been finalized and that changes and improvements are presently being incorporated. Nonetheless, as will be shown later, the model has shown good accuracy in matching temperature and pressure gradients and wellhead pressures and temperatures measured during several field tests conducted in conjunction with the model development. In its present developmental state, the model contains a number of options for the computation of friction pressure drop and holdup (hydrostatic pressure drop) in the two phase flow zone. Various combinations of these correlations have been used to obtain model results which were compared to test data. One particular set seems to have shown good consistency over a wide range of conditions and has been adopted for use in the analysis of this Roosevelt Hot Springs data.

The approach taken during formulation of the two-phase flow computer model was a logical one: the program starts with conditions of a specified flowrate, pressure and temperature at the production horizon and calculates incremental pressure drops and phase change in the fluid as it rises up the wellbore. The model also uses as input the well casing schedule and the dissolved solids and gas content of the fluid. Intermediate values of depth, pressure, temperature and steam quality are noted at specified intervals, and transistions to the different flow regimes in the two-phase region are also noted. The model has been designed with options as to the choice of two-phase pressure drop correlations that can be employed in the calculational procedure. Also, dissolved gas and solids content of the fluid can either be included in the computation or ignored. This versatility has proved to be a valuable asset in the utilization of the computer model.

The computer model was used in two ways in the analysis of the 1978 and 1979 field test information. First, the conditions measured at the production zone (pressure, temperature and flowrate) were input to the model along with the casing diameter and dissolved solids and gas content of the brine. Results of the model were then compared to the measured data acquired during the field tests. This was simply to confirm the validity of the computer program in modelling the flow for the Roosevelt Hot Springs conditions. The second application was to run through the model a parametric data set, again incorporating the fluid and reservoir parameters for the Roosevelt Hot Springs well, but varying well casing diameter and total mass flowrate. The results from this parametric data were used to predict maximum flowrates as a function of casing diameter, or for a fixed mass flowrate, the effect of a change in casing diameter on wellhead pressure. It is important to recall here that pressure drop (and thus maximum flowrate) in two-phase flows is not a simple function of fluid velocity, as in a single phase flow. The relative amounts of gas and liquid, as well as the flow regime, have a significant influence on the pressure gradient that is encountered in a wellbore flowing in a two-phase mode.

It is in this role as an accurate predictor of maximum flowrate that the two-phase model presents the greatest value to the well designer. The results shown later in this report, and more importantly, the technique developed to obtain those results, will enable the wells needed for a given installation to be optimized from a cost standpoint. For the conditions in the reservoir used as input to the model, an engineer can determine the optimum mix of number and size of wells to supply a specific quantity of fluid at given wellhead conditions, by using the model results. Furthermore, over a limited range, he can analyze the impact of changes in productivity index on his optimized system. This might be a decrease, due to scaling or reservoir depletion effects, or an increase in productivity from some type of reservoir stimulation treatment. This aspect can be of significant value under certain reservoir conditions, such as two-phase flow in the reservoir, as may be encountered in the Roosevelt KGRA.

This report presents the first case known to the authors of the use of the Two-Phase Flow computer model for optimization of wellbore designs, the purpose envisioned for the model when the development program was initiated. In particular, it is hoped that two objectives of this project are realized: first, that the information presented here will indeed be considered during the design of the Roosevelt Hot Springs geothermal utilization system, and even more important, that the technique demonstrated be adopted as a useful tool in the design and construction of geothermal systems.

To obtain the desired information of maximum flowrate for a specified wellhead pressure required some manipulation of the computer model results, since flowrate is an <u>input</u> parameter, and wellhead pressure is an output. The key to solving this problem can be found when the equations that describe the pressure drop of the system are examined. The wellhead pressure is the difference between the production horizon pressure for a given mass flow, and the pressure drop in the wellbore due to the flow, a quantity computed by the model:

$$P_{wh} = P_{pr} - \Delta P_{flow}. \tag{2}$$

However, the production pressure has already been defined in the PI equation (1):

$$P_{pr} = P_o - {}^{Q}/J;$$

combining and rearranging terms,

$$P_o - P_{wh} = \Delta P_{flow} + {}^{Q}/J \tag{3}$$

Now if a wellhead pressure is fixed at some minimum value required for a production and utilization system the above becomes:

$$\Delta P_{flow} + {}^{Q}/J = \text{constant} \tag{4}$$

For a given flowrate, the computer model will calculate the pressure drop due to flow. The value for P_o is available from analysis of the test data, and P_{wh} can be set at some representative value for the system under consideration, so that the constant on the right side of the equation is known. With the information noted, a value for J can be calculated. Additional values of Q can be input with other parameters held constant, with a corresponding change in the value of J computed for each case. These results can then be plotted to represent the maximum flowrate as a function of productivity index. The whole process can be repeated for numerous values of wellbore casing diameter, or for change in other reservoir parameters: temperature, dissolved gas content, and depth to production horizon are several good candidates. When the casing diameter is varied, the resulting series of curves presents a very graphic indication of the effect of diameter on maximum flowrate. This is easier to note when the data is manipulated further by obtaining values of Q_{max} at a fixed PI for the diameters under consideration from the Q_{max} vs J plots and replotting on a Q_{max} vs Diameter grid. The parametric data set run through the computer model has been treated exactly as described here, resulting in the graphs shown in Section IV.

IV. RESULTS AND CONCLUSIONS

A. Test Data Confirmation

Computer simulations of several of the test logs were made, to confirm the validity and accuracy of the modeling technique. Input conditions identical to the measured data from the tests were used in the computer model, and runs made for a number of correlations for the two-phase holdup (hydrostatic head) and two-phase friction contributions to the total pressure drop. Selected results of the computer simulations are shown in Figures 11 and 12.

An important discovery made early in the data analysis is shown in Figure 11. In comparing the first computer simulations to the data, it was noted that the flash horizon was predicted to be at a level of about

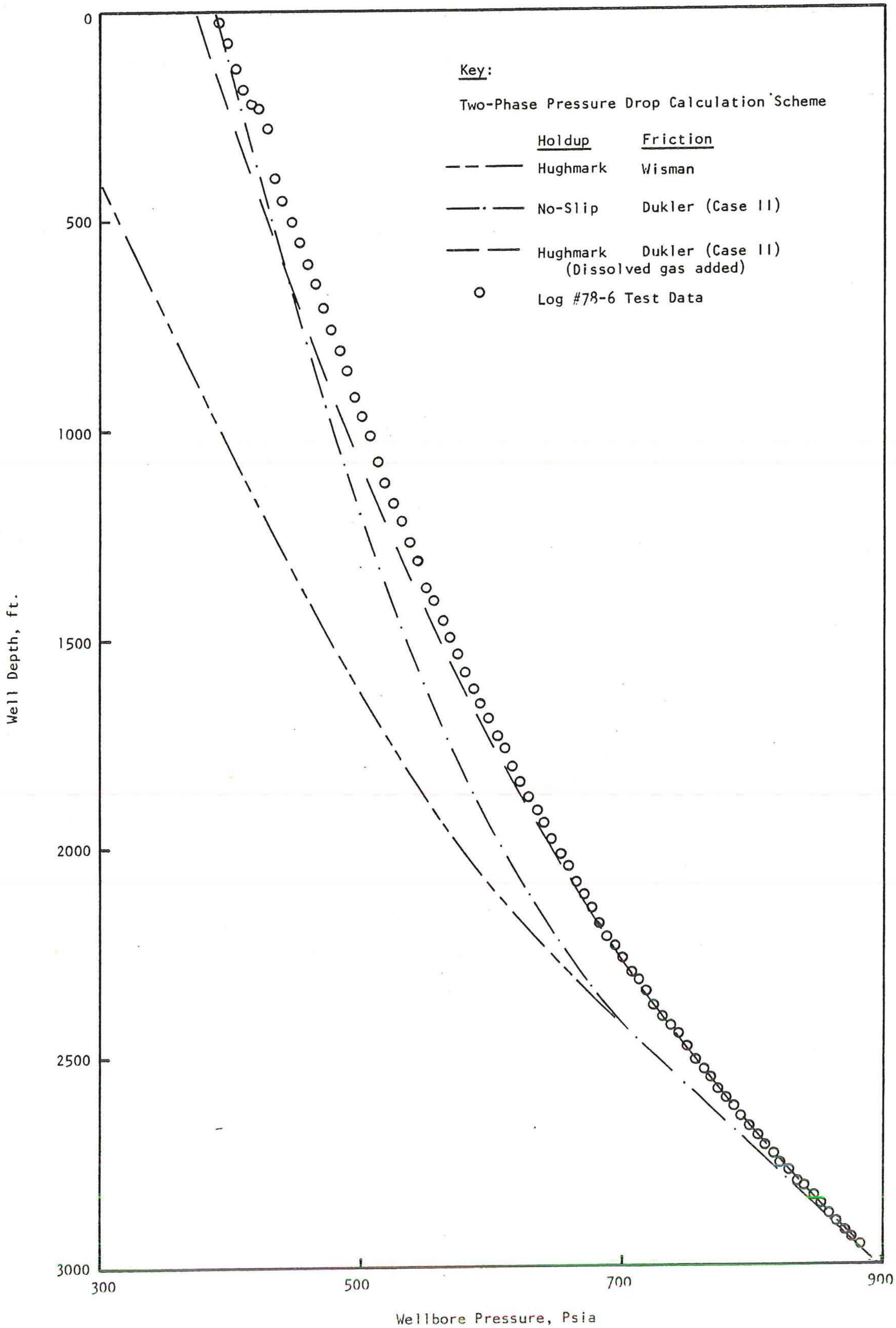

Figure II. Comparison of Computer Simulations and Measured Data for Log 78-6

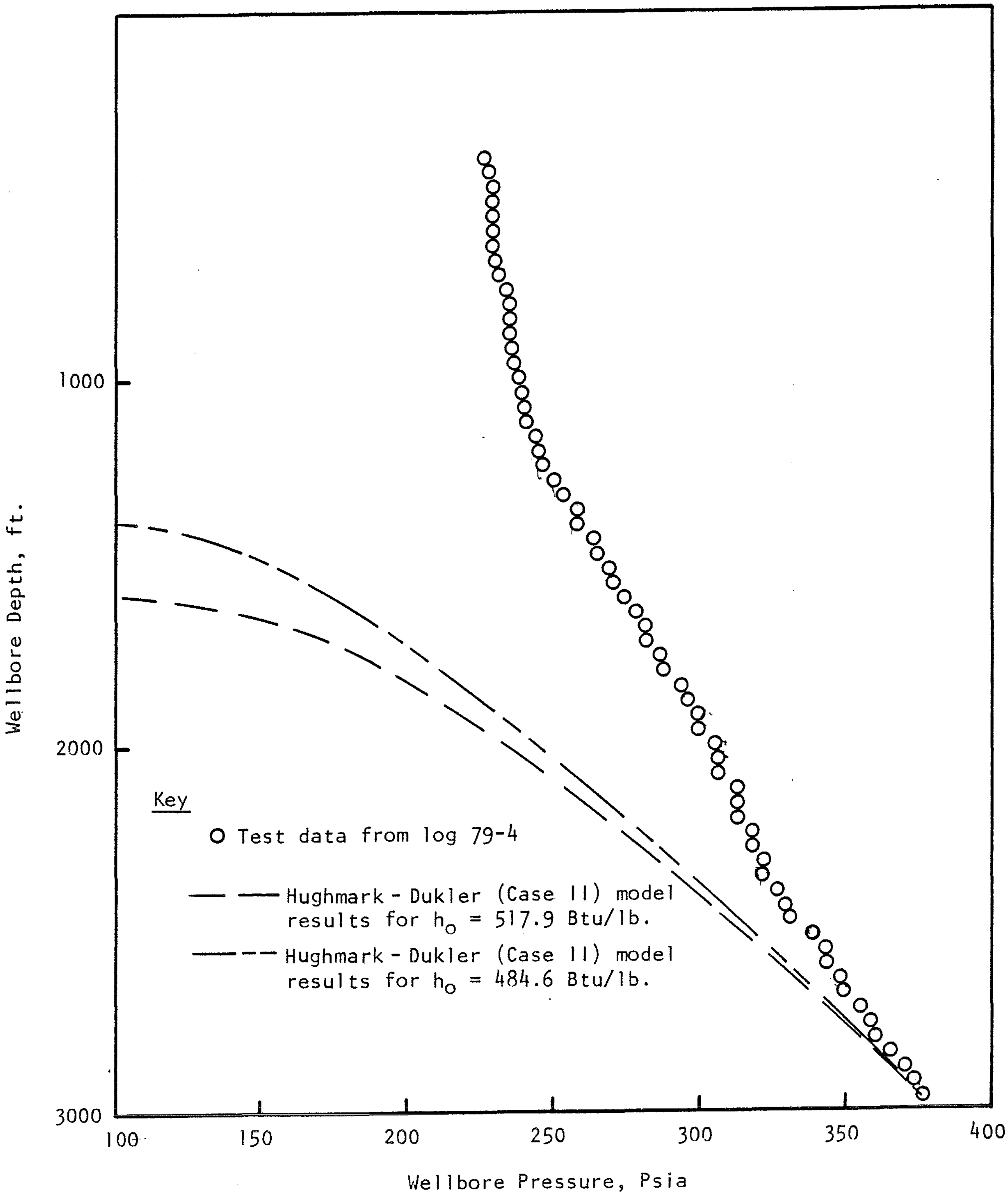

Figure 12. Comparison of Test Data and Computer Model Predictions for Log #79-4 (580,000 Lb/Hr Flowrate)

2500 ft (760 m), yet the data showed a considerable deviation from the gradient predicted for the single-phase region below this level. The single-phase pressure gradient, whose computation is straightforward, is due primarily to the effect of hydrostatic head. Since the measured deviation was toward a smaller gradient, only two possible explanations come to mind. One is that the equipment was faulty; however, all other indications were that the data was reasonable. The second explanation was that two-phase flow was beginning much deeper in the wellbore than the computer model predicted. Deeper flashing could be possible if there was an appreciable dissolved gas content in the brine. Measurements had been made of the noncondensable gases during the first field test, and indicated a content of about 0.8% of the total mass flow by weight of noncondensable gas, over 99% of which was carbon dioxide.

An additional simulation shown in Figure 11 includes the influence of the dissolved gas on the flash horizon, and the improvement in the match of the computer simulation to the test data is remarkable. There is a slight deviation in the gradient near the surface that results in an approximate 4% error in the wellhead pressure prediction; however the overall gradient match is considered excellent.

The behavior of the simulation using the No slip-Dukler (Case II) correlations merits some mention. If analysis consisted only of comparison of wellhead pressure values to measured data, the No slip-Dukler case would be considered to be an excellent representation of the flow. However, with a more careful examination of the pressure gradient, it quickly becomes obvious that it is a mere coincidence that the simulation matches the measured data at the surface; if the two-phase zone had been longer or shorter, the No slip-Dukler results would have been much less accurate.

Overall, the simulation results with the Hughmark-Dukler (Case II) model matched the test data quite well at low flowrates, when the dissolved gas content was included. This was not true at high flowrates, where the simulation results deviated significantly from the test data.

The computer model consistently predicted higher pressure drops than those measured in the tests. This discrepancy was first observed to take place when pressures at the production horizon (2950 ft or 900 m) dropped below the "flash point" value, i.e., when there existed two-phase flow in the reservoir (see Figure 12).

An examination of the literature revealed two mechanisms that would result in an increased fluid enthalpy under a two-phase flow reservoir condition. When steam exists in the formation, the relative permeability of the steam fraction may cause a preferential migration of steam to the wellbore. The result is a greater fraction of steam in the two-phase fluid than would be present due to an isenthalpic flash process. In addition, as the pressure in the reservoir drops below the flash point the temperature of the fluid also drops in accordance with the pressure/temperature saturation relationship. However, the reservoir rock matrix does not drop in temperature at the same rate as the fluid, and therefore will supply additional heat transfer to the fluid, with a resulting rise in enthalpy of the fluid in the reservoir. Eventually, heat conduction through the rock matrix will equal heat transferred to the fluid as a steady state condition is established at the reduced reservoir pressure (due to the flow from the reservoir).

A case where such conditions as described above exist in a reservoir in the Philippines has been presented at a recent conference, and an approximate 10% increase in enthalpy under the two-phase reservoir flow was noted. Coincidentally, the Philippines system resembles the Roosevelt Hot Springs reservoir under investigation here in both maximum temperature and depth to the production horizon. It was therefore decided to run addition simulation cases at a temperature that reflected an approximate 7% increase in enthalpy for the geothermal fluid since the simulated runs were at less than maximum flow. The temperature chosen was 533°F(278°C), which worked out to an enthalpy increase of about 6.9% when the effect of dissolved solids was considered.

The results of the simulations run at the higher temperature (increased enthalpy) were disappointing, as shown in Figure 12. The computed pressure gradients with the increased enthalpy cases showed even greater deviation from the data. The simulation continued to predict pressure drops much larger than those measured in the tests. This is a significant problem that must be addressed before the documentation and release of the computer model. Unfortunately, funding and time limitations did not permit additional work with the computer model as part of this contract. A point to be noted here is that the simulation results represent conservative estimates, since the predictions are for pressure drops to be greater than the values obtained during testing, for cases with high flowrates where two phase flow is suspected to occur in the reservoir.

B. Computer Model Predictions for Parametric Data Sets

A set of casing diameters and flowrates was chosen to be input to the computer model, so that an analysis of the effect of diameter change on maximum flowrate could be made for the reservoir conditions measured in the Roosevelt Hot Springs KGRA. In order to perform this analysis, a minimum value of wellhead pressure was specified to be 100 psia (689 kPa). This seemed reasonable in that sufficient pressure remains to move the fluid through a surface pipeline to a centrally located power plant and still provide a reasonable pressure drop through second stage flash tank in a dual flash cycle. In addition, for most simulation runs, when the wellbore pressure has dropped to 100 psia (689 kPa), the pressure gradient is decreasing due to the influence of acceleration pressure drop in a rapidly-evolving steam phase. This means that the computer code has reached a flow regime where large changes in pressure can occur over short lengths of wellbore.

The nature of the problem is somewhat apparent in the results noted for the test simulations in the previous section. For the high-flowrate cases, the wellhead pressures begin to approach the 100 psia (689 kPa) level and indeed the predicted pressure gradients are quite severe (shown by an almost-horizontal slope) while at the lower flowrate levels the predictions match the data quite well. In cases with larger wellbore diameters, the gradients are much smaller at the surface. This choice of wellhead pressure was somewhat arbitrary, reflecting what was thought to be a good compromise between available pressure at the wellhead for fluid transport and second stage flash, and sufficient wellbore pressure drop to maintain a large mass flowrate for the given reservoir conditions. It is important to realize that once the computer simulation runs have been made, any wellhead pressure value can be used in the calculation of productivity index for fixed values of total mass flowrate through the approach outlined in section III-D.

For the parametric cases run through the model, the results were analyzed by the method outlined in III-D to calculate a Productivity Index, J, for each set of input conditions. The reservoir temperature, depth and fluid properties (dissolved solids and gases) remained constant while the wellbore (casing) diameter and total mass flowrate were changed to provide a result which would demonstrate the effect of diameter increase in maximum flowrate for the Roosevelt Hot Springs reservoir. Six casing diameters were chosen, ranging from 7 5/8" (19.4cm) to 16" (40.6cm) outside diameter, all grade K-55 casing with weights as shown in Table 2. The table also shows maximum setting depths for the various sizes. For use in the Roosevelt Hot Springs KGRA, it is assumed that casing would be set to some intermediate depth, say 2000 ft (620m), with an open hole of approximately the same inside diameter as the casing below that level. The flowrates ranged from 300,000 lb/hr (37.9 kg/sec) to 1,000,000 lb/hr (126 kg/sec). Appropriate flowrates were assigned for each diameter, with larger flowrates being run with larger diameter casing.

Curves showing the relationship between flowrate and productivity index, J, are shown for the diameters under investigation in Figure 13. The data for the 7 5/8" casing diameter curve includes a point used in determining the shape which lies off the scale shown in the Figure. The information in Figure 13 was derived from computer simulations that assumed a fluid enthalpy of 484.6 Btu/lb (1127 kilojoules/kilogram). The increase in flowrate with increase in productivity index is explained

TABLE 2

CASING DESIGN LIMITS, LARGE DIAMETER CASING

Casing Outside Diameter (inches)	Casing Weight (lb/ft)	Maximum Length Collapse (ft)	Maximum Length Tension Failure (ft)	Maximum Length Internal Burst (ft)
7 5/8	26.4	5140	12230	8280
9 5/8	36	3590	11650	7040
10 3/4	45.5	3720	11370	7160
11 3/4	54	3680	11100	7120
13 3/8	61	2740	10650	6180
16	84	2510	9910	5960
		Limiting Value For All Sizes		

NOTES: Safety factors:

Collapse	1.125
Tension	1.8
Burst	1.0 (of minimum internal yield pressure)

Bottom Hole Pressure for collapse computed for 9.625 ppg mud

Tension failure assumes regular buttress thread coupling

All casing is grade K-55

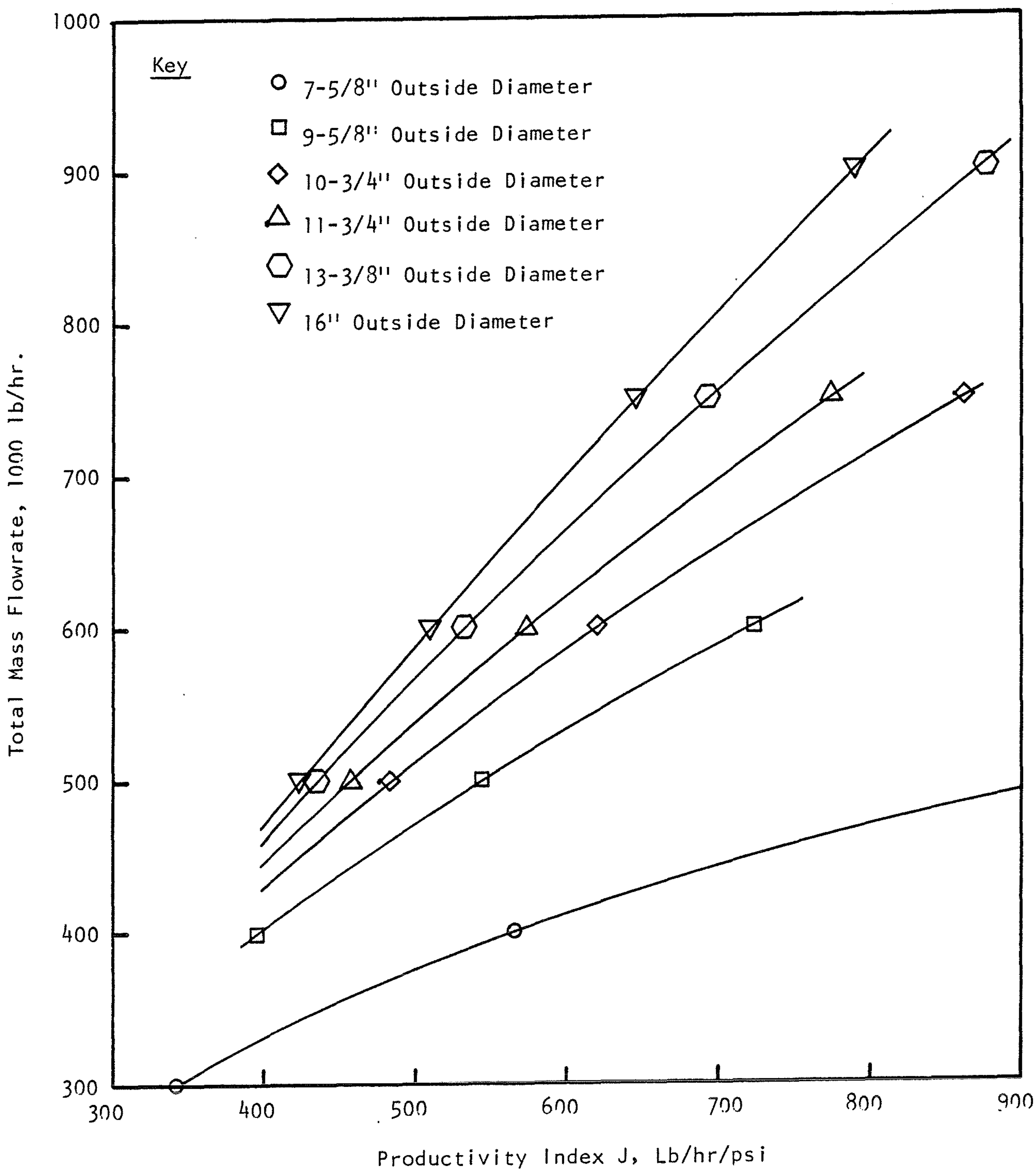

Figure 13. Computer Model Results of Flowrate vs. Productivity Index for h_o = 484.6 Btu/lb.

by noting that as J becomes larger, the portion of the total pressure drop due to drawdown remains constant only if total mass flow is increased (see equation (3)). This concept may be easier to understand if the distribution of the available pressure drop is graphed for a typical case. Figure 14 presents such a distribution of pressure drop as a function of productivity index for 9 5/8 inch (24.4 cm) diameter casing. This is simply a plot of distribution of the available pressure drop as a function of productivity index. The important result here is that as J increases, the drawdown component of the total pressure drop becomes smaller, a point whose significance will be noted shortly.

The graph of total mass flowrate as a function of productivity index can now be used to construct a second graph which shows the effect of a change in casing diameter on the total mass flowrate at a constant productivity, the situation which would be encountered when designing production wells for a known field. In addition, data can be obtained for productivities greater than or less than the known value, to permit a sensitivity analysis of the results to be performed. The data points needed for construction of the graph of maximum total flowrate as a function of casing diameter are found simply by following a line of the constant productivity index (this would be a vertical line on Figure 13) of interest to its intersection with curves for each of the diameters.

For the case of "Utah State" 14-2, the results of such a procedure are presented in Figure 15. As noted earlier, the productivity index for this well, calculated from field test data, is 589 lb/hr-psi (5.22×10^{-2} kg/sec-kPa). Also plotted are data for two additional productivity indices J = 400 lb/hr-psi (3.54×10^{-2} kg/sec-kPa) and J = 750 lb/hr-psi (6.65×10^{-2} kg/sec-kPa). These additional data are provided for two purposes: first, to demonstrate how the productivity index parameter affects the increase in maximum total mass flowrate with increasing casing diameter, and second to present an indication of expected well performance if a change in productivity index occurs. For example, a decrease in productivity index may be attributable to scaling in the reservoir when two-phase flow is found there, as is suspected at high

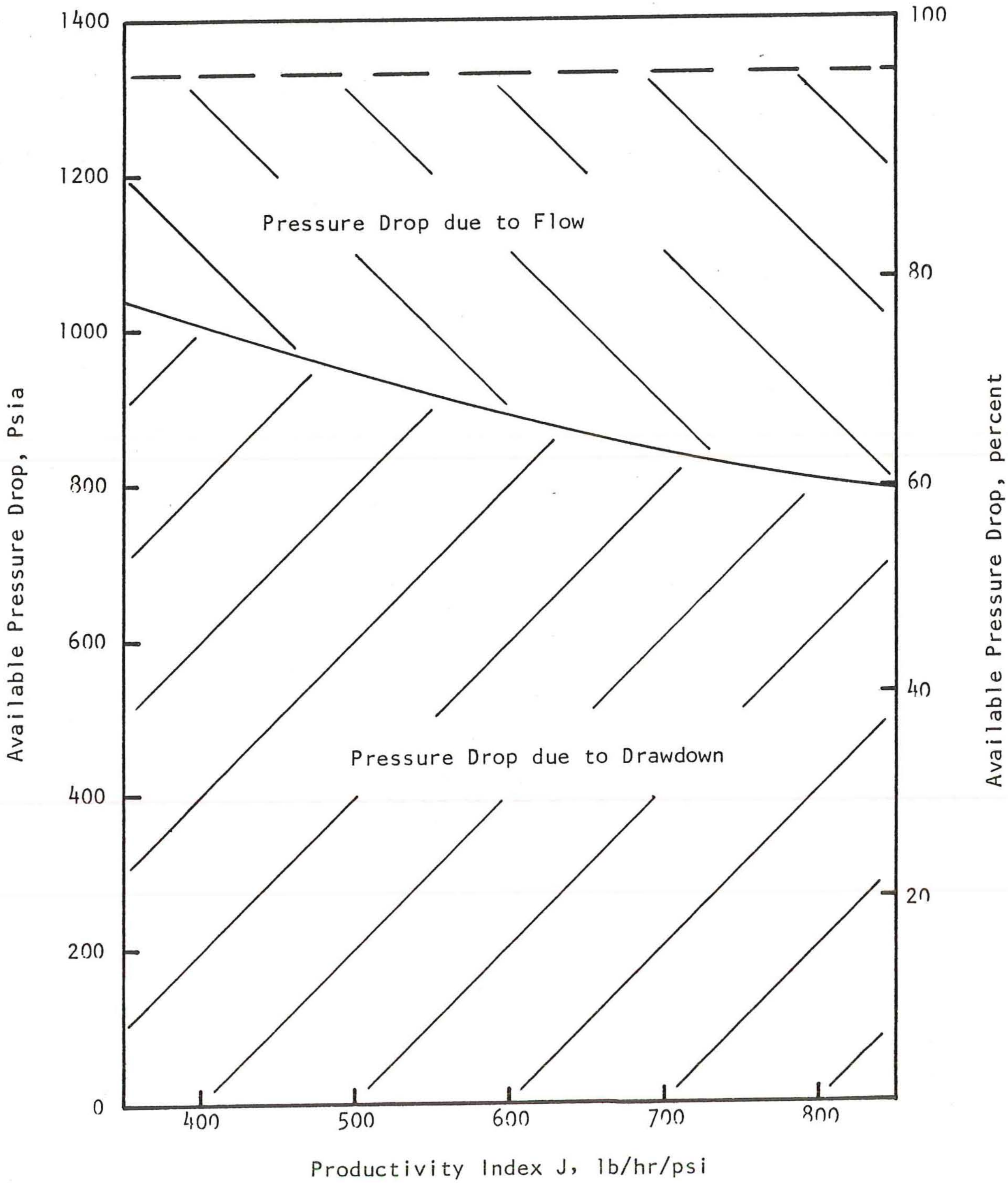

Figure 14. Pressure Drop Distribution for 9-5/8 Inch Diameter Casing

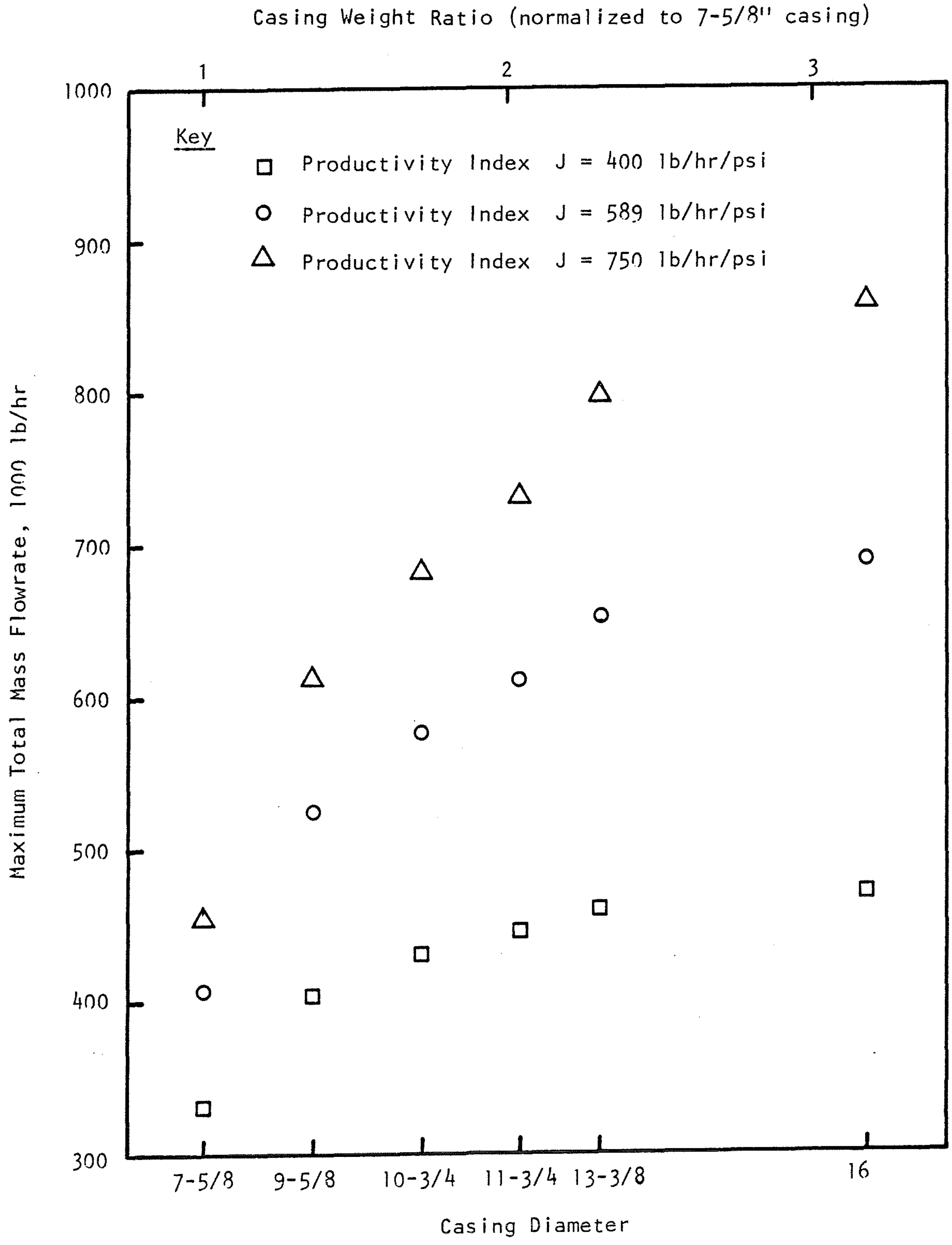

Figure 15. Computed Maximum Flowrate as a Function of Casing Diameter and Productivity Index

flowrates in "Utah State" 14-2. An increase in productivity index could be caused by a successful well stimulation treatment or even through more careful well completion practices so as to avoid "skin damage" problems.

The effect of productivity index on the data plotted in Figure 15 can now be related to the distribution of the total pressure drop which was detailed in Figure 14. Casing diameter changes can directly influence only the pressure drop due to flow so that when the flow pressure drop is only a small portion of the total (at a low productivity index), reduction in the flow pressure drop can only have a small effect on the total pressure drop. At greater values of the productivity index, the flow pressure drop makes a greater relative contribution to the total and therefore reduction in the flow pressure drop in larger diameter casing can provide for a significant increase in flowrate (i.e. since the total pressure drop is constant, a smaller flow contribution means that a larger drawdown contribution is possible, reflected by a greater flowrate).

The abscissa (diameter axis) in Figure 15 is plotted in a scale of relative casing weight (on a per-foot basis). All values were normalized via division by the weight of 7 5/8 inch (19.4 cm) diameter casing. This was done with the thought that to a first-order approximation, the relative cost of well casing will be the same as the relative weight.

With the data presented in Figure 15 and a knowledge of the contributions of casing, cementing and drilling costs as a function of diameter to the total cost of a well, it is possible to determine an optimum well diameter and flowrate. The tradeoff to be evaluated becomes one of increased cost for larger diameter casing versus the increased production that the larger diameter casing affords. This can be extended to all wells planned for a particular field so that the total required mass flowrate can be appportioned over a number of wells, with the thought that due to increased well performance via optimization of the two-phase pressure drop, one or more production wells may be eliminated.

A second graph of total mass flowrate as a function of productivity index was also developed from an additional set of parametric computer simulation data. These runs were made with an input reservoir temperature of 544^{o}F (284.4^{o}C) so that the enthalpy of the fluid in the wellbore would be about 10% greater than the earlier simulations, run at 505^{o}F (262.8^{o}C). This enthalpy gain was postulated to be due to flash in the reservoir, as described earlier (section IV-A). The results are presented in Figure 16, whose close examination will reveal that all data points are within about 2% of similar values at the lower enthalpy rate. The question raised by this lack of change is whether it is a true and dependable result or whether it is just an artifact of the particular correlations used in calculation of the two-phase pressure drop. Unfortunately, a detailed investigation of the answer lies beyond the scope of this study.

However, with the information available from the field tests, one check on the validity of the results of the computer simulations is possible. With known wellhead pressures for each of the computed well flowrates from both the 1978 and 1979 test series, a least squares quadratic equation has been formulated. The data and resulting equation are presented in Table 3; the correlation coefficient for the least squares quadratic was 0.907 which indicates a quite good fit of the data to the approximating equation. When the wellhead minimum pressure of 100 psia (689 kPa) used in the simulations is inserted into the quadratic, a total mass flowrate of 605,000 lb/hr (76.4 kg/sec) is calculated. This is about 15% larger than the 525,000 lb/hr (66.3 kg/sec) maximum total mass flowrate predicted by the computer model for 9 5/8 in (24.4 cm) diameter casing. Of course, the quadratic results are a projection based on data taken at lower flowrates, so that a 15% error may be considered reasonable. Also, the accuracy of the flowrate measurements via the James method is no better than within 15% of the actual value.

One last result of the computer simulation work merits mention here. Figure 17 demonstrates the effect of increase in casing diameter on wellhead pressure at a constant flowrate, in this example, for 500,000

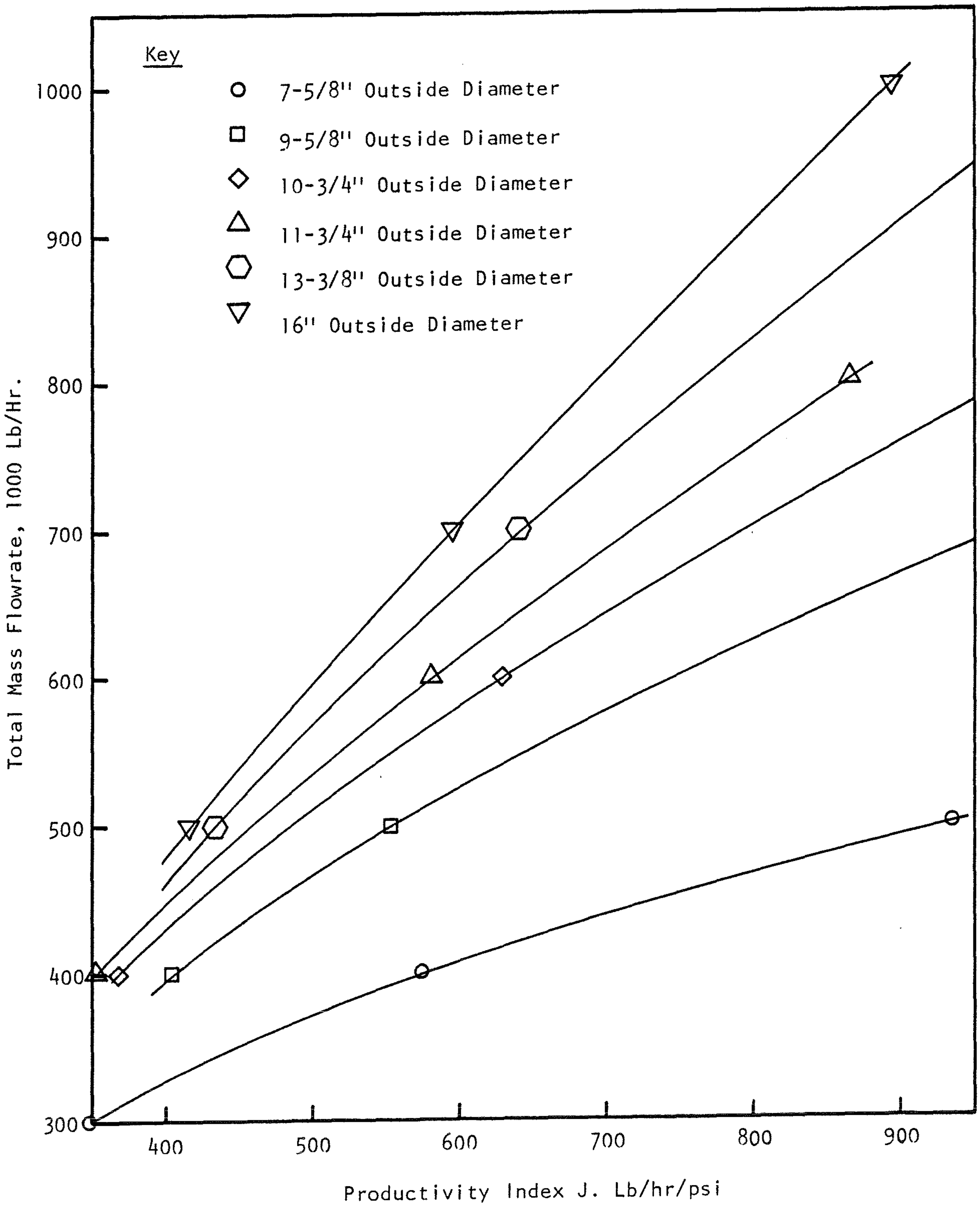

Figure 16. Computer Model Results of Flowrate vs. Productivity Index for h_o = 531.4 Btu/Lb.

TABLE 3

"Utah State" 14-2 Wellhead Pressure vs Flowrate Information

Log No.	P_{wh} (psia)	Q (lb/hr)
79-1	449	284,000
79-2	433	325,000
79-3	258	505,000
79-4	172	580,000
79-5	266	443,000
78-2	379	357,000
78-3	354	454,000
78-5	441	255,000
78-6	391	369,000

Least squares quadratic fit of above data:

$$Q = 635,372-166.16\ P_{wh}-1.3854\ (P_{wh})^2$$

or, if 100 psia minimum wellhead pressure is assumed:

$$Q_{max} = 604902 \text{ lb/hr at 100 psia}$$

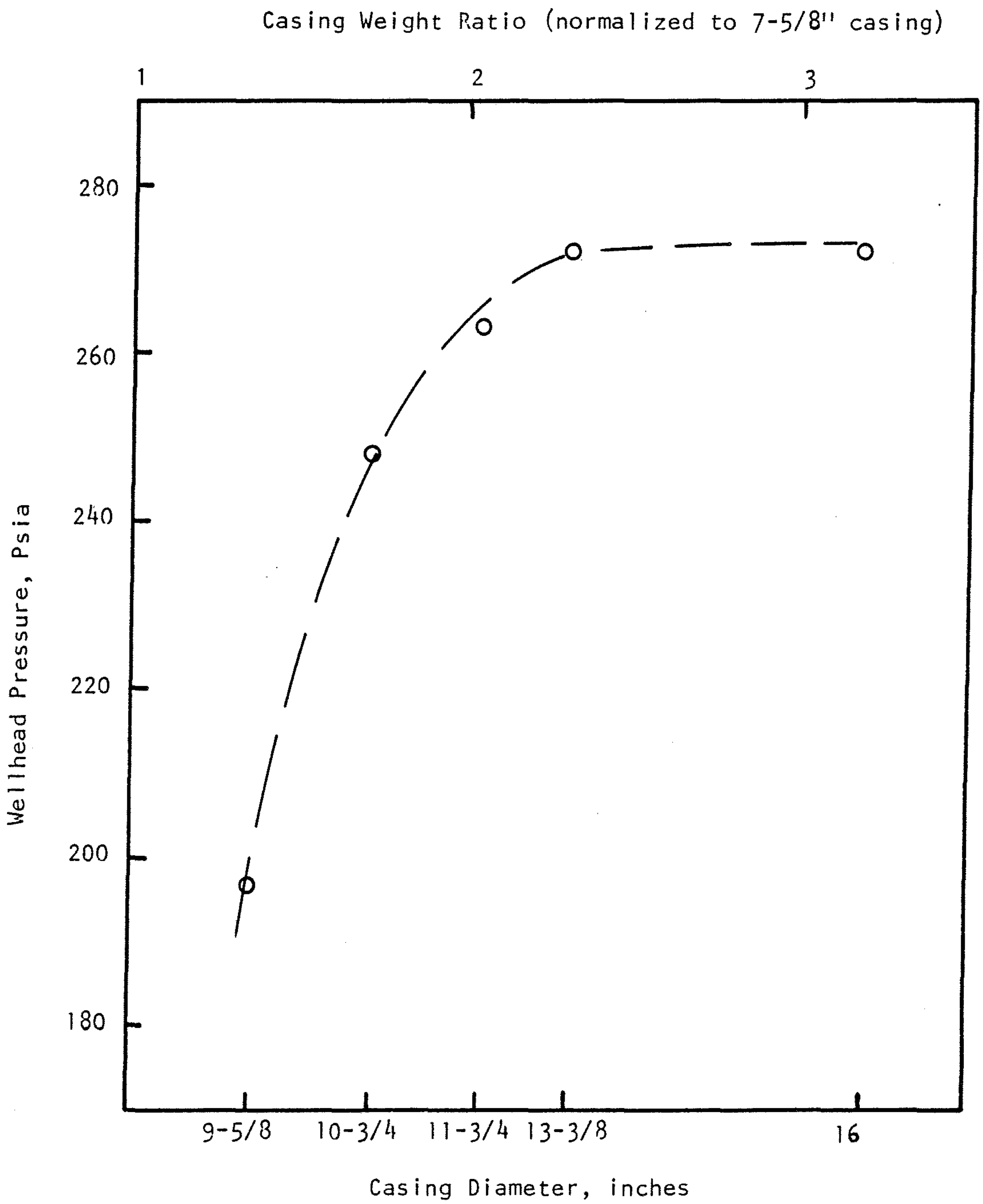

Figure 17. Wellbore Pressure Drop (as Reflected by Wellhead Pressure) as a Function of Casing Diameter for a Flow of 500,000 Lb/Hr.

lb/hr (63.1 kg/sec). The significant point is that the increase diminishes with each succeeding diameter and that between the two largest casing sizes considered, there is no change at all! Since a further pressure reduction would probably occur in a first stage flash tank, a legitimate question would seem to be: why worry about wellhead pressure so long as it is sufficient to move the fluid through the surface gathering lines to the first stage flash tank in a plant?

There is a good reason to worry about wellhead pressure, and it involves the mechanics of scale formation in the well. When pressure drops below the saturation level for dissolved gases (especially carbon dioxide), they begin to come out of solution and form a gas phase. This dissolution action causes a shift in pH and in turn unbalances the dissolved solids chemical equilibrium in the fluid. Solids then begin to precipitate as scale in the wellbore. If pressure drop in the wellbore is maintained at a minimum level, (i.e. high wellhead pressure maintained for a constant flowrate), the scaling downhole will be kept to a minimum, with some of the scale formation occurring in surface lines and equipment, where the problem is much easier to control.

C. Conclusions

Logs of pressure and temperature as a function of depth have been obtained from well "Utah State 14-2" at Roosevelt Hot Springs KGRA, Utah. The data was taken while the well was flowing at rates up to 580,000 lbs/hr (73 kg/sec). Maximum recorded value of temperature was 503°F (262°C) and pressure, 954 psia (6.6 MPa). This information was used to determine certain well performance parameters and was compared to computer simulations made with identical input conditions in order to validate the operation of the computer model.

A technique for the reduction of computer simulation data to a form where the performance of various wellbore diameters can be compared has been developed and demonstrated. When reservoir properties are known, well design can be optimized from both cost and performance aspects.

The correlations employed in the computer model have been demonstrated to model test data quite accurately at flowrates up to 300,000 lbs/hr (38 kg/sec) but seem to show proportionately greater deviation from test results as flowrates increase above that level. This deviation is thought to be due to initiation of flashing and accompanying two-phase flow in the reservoir at high flowrates. However, this problem does not invalidate the computer technique; rather, it indicates that additional development work on the computer modelling is necessary. Confirmation of this conclusion rests in the resulting model predictions which show a good agreement with extrapolations of field test data.

The results of application of the developed predictive technique to the Roosevelt Hot Springs reservoir conditions are noteworthy. The effect of both wellbore diameter and preductivity index on maximum well flowrates is shown to be significant. For example, a 24% increase in total mass flowrate is predicted if 13 3/8 inch (34.0 cm) casing is used instead of the current 9 5/8 inch (24.4 cm) casing. The wellhead pressure maintained by both flows is equal, and thus the number of wells required to support a given development is reduced. The impact of this type of optimization on project economics is obvious.

The conditions known to exist in the Roosevelt Hot Springs KGRA are such that commercial production there will require two-phase flow in the wellbores. Further, it is suspected that at high flowrates the two-phase flow region will extend into the reservoir itself. Indeed, some investigators predict that a steam cap may form in the reservoir over some long period of time. Certainly such activity will affect the pressure, temperature and enthalpy of fluid at entrance to the wellbore, three parameters which impact the two-phase flow pressure drop. Again, if some quantitative predictions of these changes can be made, the technique shown in this report can be used to predict resulting well performance.

The analysis given here can be applied and extended in a number of directions, and the questions raised in the preparation of this report suggest several. The effect of two-phase reservoir flow on the two-phase flow up the wellbore deserves to be investigated further. The impact of dissolved gases on the saturation pressure and onset of two-phase was significant, an area where additional well test data may prove to be quite valuable. Also, the sensitivity of the computer simulation to such variables as fluid enthalpy and total mass flowrate should be explored further.

The information presented in this report should become quite useful in the design of the production field for the Roosevelt Hot Springs KGRA, and hopefully will be extended to the optimization of other hydrothermal development projects.

APPENDIX A

TABLE A1.1978 Test Data

Log No. 78-2 Flow Rate 357,000 lbs/hr. (?)

TPC/AMAX Well 14-2

Depth (ft)	Transducer Count (No. of Steps)	Pressure (psia)	Depth (ft)	Transducer Count (No. of Steps)	Pressure (psia)
49		379	1713	31	573
118	0 (reference)	385	1752	32	579
178	1	391	1793	33	585
237	2	397	1821	34	591
314	3	403	1853	35	597
382	4	409	1898	36	603
409	5	415	1932	37	609
430	6	421	1966	38	615
486	7	427	2001	39	621
608	8	433	2028	40	627
663	9	440	2059	41	633
728	10	446	2090	42	640
779	11	452	2129	43	646
832	12	458	2163	44	652
878	13	464	2188	45	658
939	14	470	2223	46	664
990	15	476	2250	47	670
1036	16	482	2280	48	676
1086	17	488	2313	49	682
1140	18	494	2342	50	688
1178	19	500	2359	51	694
1229	20	506	2386	52	700
1283	21	512			
1329	22	518			
1370	23	524			
1412	24	530			
1459	25	537			
1508	26	543			
1545	27	549			
1594	28	555			
1634	29	561			
1676	30	567			

Comments:

Flowrate value seems low for given wellhead pressure

TABLE A1. 1978 Test Data (Continued)

Log No. 78-3

Flow Rate 447,500 lbs/hr.

TPC/AMAX Well 14-2

Depth (ft)	Transducer Count (No. of Steps)	Pressure (psia)	Depth (ft)	Transducer Count (No. of Steps)	Pressure (psia)
50	0 (reference)	355	2032	32	549
134	1	361	2076	33	555
239	2	367	2122	34	561
324	3	373	2167	35	567
380	4	379	2213	36	573
452	5	385	2255	37	579
529	6	391	2283	38	585
597	7	397	2337	39	591
615	8	403	2374	40	597
641	9	410	2415	41	603
702	10	416	2455	42	610
846	11	422	2490	43	616
913	12	428	2525	44	622
978	13	434	2560	45	628
1063	14	440	2606	46	634
1125	15	446	2643	47	640
1180	16	452	2672	48	646
1249	17	458	2711	49	652
1300	18	464	2746	50	658
1353	19	470	2781	51	664
1410	20	476	2820	52	670
1470	21	482	2855	53	676
1515	22	488	2873	54	682
1568	23	494	2901	55	688
1634	24	500	2950	56	694
1686	25	507	2964	57	700
1733	26	513	2990	58	707
1784	27	519			
1834	28	525			
1883	29	531			
1933	30	536			
1982	31	543			

Comments:
Suspect flashing in formation

TABLE A1. 1978 Test Data (Continued)

Log No. 78-4 Flow Rate 255,000 lbs/hr.

TPC/AMAX Well 14-2

Depth (ft)	Transducer Count (No. of Steps)	Pressure (psia)	Depth (ft)	Transducer Count (No. of Steps)	Pressure (psia)
12	0 (reference)	435	1575	33	635
70	1	441	1610	34	641
118	2	447	1642	35	647
162	3	453	1686	36	653
216	4	459	1721	37	659
264	5	465	1748	38	665
312	6	471	1786	39	671
360	7	477	1822	40	677
414	8	483	1862	41	683
457	9	490	1897	42	690
515	10	496	1937	43	696
558	11	502	1959	44	702
606	12	508	1994	45	708
664	13	514	2042	46	714
716	14	520	2065	47	720
769	15	526	2095	48	726
820	16	532	2131	49	732
861	17	538	2170	50	738
922	18	544	2205	51	744
974	19	550	2245	52	750
1015	20	556	2274	53	756
1067	21	562	2322	54	762
1118	22	568	2366	55	768
1163	23	574	2398	56	774
1213	24	580	2446	57	780
1258	25	587	2489	58	787
1300	26	593	2540	59	793
1328	27	599	2577	60	799
1374	28	605	2634	61	805
1421	29	611	2688	62	811
1464	30	617	2770	63	817
1505	31	623	2932	64	823
1544	32	629	2994	65	829

Comments: Log taken before flow completely stabilized. Values in lower part of wellbore are particularly suspect. Log made from 3000' level upward.

TABLE A1. 1978 Test Data (Continued)

Log No. 78-5 Flow Rate 255,000 lbs/hr.

TPC/AMAX Well 14-2

Depth (ft)	Transducer Count (No. of Steps)	Pressure (psia)	Depth (ft)	Transducer Count (No. of Steps)	Pressure (psia)
52	0 (reference)	441	1473	33	641
98	1	447	1502	34	647
142	2	453	1542	35	653
208	3	459	1572	36	659
259	4	465	1596	37	665
297	5	471	1634	38	671
350	6	477	1660	39	677
410	7	483	1693	40	683
444	8	489	1723	41	689
494	9	496	1758	42	696
549	10	502	1775	43	702
583	11	508	1804	44	708
633	12	514	1844	45	714
687	13	520	1858	46	720
738	14	526	1878	47	726
777	15	532	1908	48	732
822	16	538	1933	49	738
866	17	544	1962	50	744
911	18	550	1983	51	750
960	19	556	2008	52	756
1004	20	562	2032	53	762
1043	21	568	2057	54	768
1088	22	574			
1122	23	580			
1162	24	586			
1205	25	593			
1235	26	599			
1265	27	605			
1306	28	611			
1340	29	617			
1376	30	623			
1410	31	629			
1442	32	635			

Comments:

TABLE A1. 1978 Test Data (Continued)

Log No. 78-6

Flow Rate 368,800 lbs/hr.

TPC/AMAX Well 14-2

Depth (ft)	Transducer Count (No. of Steps)	Pressure (psia)	Depth (ft)	Transducer Count (No. of Steps)	Pressure (psia)
32	0 (reference)	391	1624	32	585
70	1	397	1657	33	591
134	2	403	1694	34	597
188	3	409	1736	35	603
222	4	415	1769	36	609
230	5	421	1809	37	615
280	6	427	1844	38	621
400	7	433	1880	39	627
456	8	439	1913	40	633
505	9	446	1946	41	639
554	10	452	1986	42	646
610	11	458	2020	43	652
654	12	464	2048	44	658
718	13	470	2087	45	664
764	14	476	2116	46	670
812	15	482	2149	47	676
867	16	488	2187	48	682
924	17	494	2215	49	688
972	18	500	2237	50	694
1016	19	506	2267	51	700
1078	20	512	2301	52	706
1129	21	518	2320	53	712
1177	22	524	2348	54	718
1221	23	530	2380	55	724
1272	24	536	2408	56	730
1320	25	543	2430	57	736
1378	26	549	2450	58	743
1412	27	555	2478	59	749
1460	28	561	2512	60	755
1500	29	567	2534	61	761
1539	30	573	2552	62	767
1584	31	579	2580	63	773

Comments:

TABLE A1.1978 Test Data (Continued)

Log No. 78-7 Flow Rate 368,800 lbs/hr.

TPC/AMAX Well 14-2

Depth (ft)	Transducer Count (No. of Steps)	Pressure (psia)	Depth (ft)	Transducer Count (No. of Steps)	Pressure (psia)
2601	64	779			
2624	65	785			
2647	66	791			
2670	67	797			
2690	68	803			
2715	69	809			
2732	70	815			
2754	71	821			
2774	72	827			
2804	73	833			
2814	74	839			
2832	75	846			
2855	76	852			
2878	77	858			
2899	78	864			
2922	79	870			
2936	80	876			
2955	81	882			
2979	82	888			
2996	83	894			

Comments:

TABLE A2. 1979 Test Data

Log No. 79-2

Flow Rate 325,000 lb/hr

TPC/AMAX Well 14-2

Depth (ft)	Temperature (°F)	Pressure (psia)	Depth (ft)	Temperature (°F)	Pressure (psia)
80	453.25	446	1280	474.5	568
120	453.25	448	1320	475.25	573
160	453.75	451	1360	476.0	579
200	454.0	454	1400	476.75	584
240	454.5	457	1440	477.5	589
280	455.0	460	1480	478.0	594
320	455.5	462	1520	478.75	600
360	456.0	463	1560	479.75	609
400	456.75	468	1600	480.5	615
440	457.5	471	1640	481.25	623
480	458.5	476	1680	482.0	628
520	459.25	482	1720	482.75	634
560	460.0	-	1760	483.5	645
600	461.0	-	1800	484.5	651
640	461.75	494	1840	485.25	658
680	462.5	498	1880	486.25	665
720	463.25	500	1920	487.0	671
760	464.0	503	1960	487.5	682
800	464.75	508	2000	488.5	690
840	465.5	510	2040	489.25	700
880	466.5	519	2080	489.75	707
920	467.25	524	2120	490.5	721
960	467.75	527	2160	491.25	730
1000	468.75	533	2200	492.0	736
1040	469.75	539	2240	493.0	745
1080	470.5	543	2280	493.5	756
1120	471.25	545	2320	494.25	765
1160	472.0	550	2360	494.75	776
1200	472.75	556	2400	495.25	786
1240	473.5	561	2440	496.0	795

Comments:

Flowrate average shown above is based on 8 data points. Computed standard deviation is 12,000 lb/hr, or a normalized value of 0.037. Accuracy of the James method measurement technique is estimated at ± 15%.

TABLE A2. 1979 Test Data (Continued)

Log No. 79-2 (concluded) Flow Rate 325,000 lb/hr

TPC/AMAX Well 14-2

Depth (ft)	Temperature (°F)	Pressure (psia)	Depth (ft)	Temperature (°F)	Pressure (psia)
2480	496.5	807			
2520	497.0	814			
2560	497.5	826			
2600	498.0	838			
2640	498.5	850			
2680	499.0	857			
2720	499.5	867			
2760	499.75	876			
2800	500.25	889			
2840	500.5	901			
2880	501.0	914			
2920	501.25	924			
2960	502.5	937			
3000	503.0	954			

Comments:

TABLE A2. 1979 Test Data (Continued)

Log No. 79-4

Flow Rate 580,000 lb/hr

TPC/AMAX Well 14-2

Depth (ft)	Temperature (°F)	Pressure (psia)	Depth (ft)	Temperature (°F)	Pressure (psia)
400	397.25	227	1600	411.0	274
440	397.5	228	1640	412.0	278
480	397.75	229	1680	413.0	282
520	398.0	228	1720	414.25	282
560	398.0	228	1760	415.0	287
600	398.25	229	1800	416.0	288
640	398.5	229	1840	417.0	294
680	398.75	230	1880	417.5	296
720	399.0	232	1920	418.0	299
760	399.25	234	1960	418.75	299
800	399.5	235	2000	419.25	305
840	399.75	235	2040	420.0	307
880	400.0	235	2080	420.75	307
920	400.25	236	2120	421.25	313
960	400.75	237	2160	422.0	313
1000	401.5	238	2200	422.5	313
1040	402.0	239	2240	423.25	318
1080	402.25	240	2280	424.0	318
1120	402.5	241	2320	424.5	322
1160	403.0	244	2360	425.25	322
1200	403.5	245	2400	426.25	327
1240	404.25	247	2440	426.75	329
1280	405.25	251	2480	427.5	331
1320	405.75	254	2520	428.75	339
1360	406.75	258	2560	429.5	343
1400	407.5	258	2600	430.25	343
1440	408.25	264	2640	431.0	348
1480	409.0	265	2680	431.75	349
1520	409.75	269	2720	432.5	355
1560	410.25	271	2760	433.25	358

Comments:

Flowrate average shown above is based on 12 data points. Computed standard deviation is 39,400 lb/hr., or a normalized value of 0.068. Accuracy of the James method measurement technique is estimated at ± 15%.

TABLE A2. 1979 Test Data (Continued)

Log No. 79-4 (Continued) Flow Rate 580,000 lb/hr

TPC/AMAX Well 14-2

Depth (ft)	Temperature (°F)	Pressure (psia)	Depth (ft)	Temperature (°F)	Pressure (psia)
2800	434.25	360	4000	452.75	453
2840	435.0	365	4040	453.25	456
2800	436.0	370	4080	453.5	456
2920	436.75	373	4120	453.75	463
2960	437.5	376	4160	454.5	463
3000	438.25	380	4200	455.0	469
3040	439.0	382	4240	455.5	472
3080	440.0	383	4280	455.5	469
3120	440.75	385	4320	456.25	469
3160	441.5	390	4360	456.75	472
3200	442.0	400	4400	457.25	480
3240	442.75	403	4440	458.0	486
3280	443.25	410	4480	458.5	487
3320	443.75	410	4520	459.0	490
3360	444.25	410	4560	459.75	492
3400	444.75	410	4600	460.25	496
3440	445.5	413	4640	460.75	502
3480	446.0	414	6480	461.5	504
3520	446.5	419	4720	462.0	510
3560	447.5	420	4760	462.5	513
3600	448.0	426	4800	463.25	519
3640	448.5	427	4840	464.0	522
3680	449.0	430	4880	464.5	526
3720	449.5	432	4920	465.0	528
3760	450.0	437	4960	465.5	530
3800	450.75	440	5000	466.25	535
3840	451.0	446	5040	466.75	539
3880	451.5	447	5080	467.25	542
3920	451.75	450	5120	468.0	549
3960	452.25	453	5160	468.25	554

Comments:

TABLE A2. 1979 Test Data (Continued)

Log No. 79-4 (concluded) Flow Rate 580,000 lb/hr

TPC/AMAX Well 14-2

Depth (ft)	Temperature (°F)	Pressure (psia)	Depth (ft)	Temperature (°F)	Pressure (psia)
5200	468.75	555			
5240	469.25	562			
5280	470.0	566			
5320	470.5	573			
5360	471.0	579			
5400	471.5	586			
5440	472.0	589			
5480	472.5	591			
5520	473.0	597			
5560	473.75	602			
5600	474.25	610			
5640	474.75	613			
5680	475.25	626			
5720	476.0	629			
5760	476.5	635			
5800	477.25	638			
5840	478.0	648			
5880	478.5	653			
5920	480.0	665			
5960	483.0	676			
6000	484.25	688			
6040	488.0	696			
6060	488.75	710			

Comments:

TABLE A2. 1979 Test Data (Continued)

Log No. 79-5 Flow Rate 443,000

TPC/AMAX Well 14-2

Depth (ft)	Temperature (°F)	Pressure (psia)	Depth (ft)	Temperature (°F)	Pressure (psia)
520	423.5	322	1720	442.5	416
560	424.25	324	1760	443.75	421
600	425.0	327	1800	444.25	422
640	425.5	328	1840	444.75	427
680	426.25	333	1880	445.25	432
720	426.75	335	1920	446.25	435
760	427.5	340	1960	446.75	439
800	428.0	342	2000	447.25	439
840	428.75	347	2040	448.0	445
880	429.25	349	2080	449.0	448
920	430.0	350	2120	449.75	454
960	430.5	353	2160	450.5	460
1000	431.25	358	2200	451.25	461
1040	432.0	360	2240	451.75	465
1080	432.5	366	2280	452.25	471
1120	432.75	367	2320	453.0	473
1160	433.5	368	2360	454.0	479
1200	434.0	369	2400	454.25	483
1240	434.5	370	2440	454.5	484
1280	434.5	374	2480	455.0	486
1320	435.0	376	2520	455.25	491
1360	435.5	380	2560	455.5	489
1400	435.75	381	2600	456.0	492
1440	436.25	388	2640	456.25	500
1480	437.25	390	2680	456.5	501
1520	437.75	394	2720	457.0	502
1560	438.5	400	2760	457.25	502
1600	439.75	412	2800	457.5	504
1640	440.5	415	2840	457.5	505
1680	441.25	416	2880	457.75	506

Comments:

Flowrate average shown above is based on 11 data points. Computed standard deviation is 49,000 lb/hr., or a normalized value of 0.111. This wide deviation is due to a shift in throttle valve position from unknown causes during logging. Upon discovery the valve was reset to its original position. Accuracy of the James method measurement technique is estimated at ± 15%.

TABLE A2. 1979 Test Data (Continued)

Log No. 79-5 (concluded) Flow Rate 443,000 lb/hr

TPC/AMAX Well 14-2

Depth (ft)	Temperature (°F)	Pressure (psia)	Depth (ft)	Temperature (°F)	Pressure (psia)
2920	458.5	511	4120	474.0	646
2960	458.5	512	4160	474.5	652
3000	458.75	512	4200	475.0	662
3040	458.75	512	4240	475.0	667
3080	458.75	513	4280	475.25	680
3120	459.0	515	4320	475.75	686
3160	459.5	520	4360	476.0	696
3200	460.0	524	4400	476.5	703
3240	460.75	529	4440	478.0	714
3280	461.25	534	4480	478.5	722
3320	461.75	538	4520	479.25	731
3360	462.5	542	4560	480.0	736
3400	463.0	545	4600	480.5	749
3440	463.75	550	4640	481.0	760
3480	464.25	557	4680	481.5	766
3520	465.0	558	4720	481.75	776
3560	465.25	566	4760	481.75	784
3600	466.0	573	4800	482.0	792
3640	466.5	476	4840	481.0	808
3680	467.25	479	4880	481.25	815
3720	467.75	587	4920	480.75	836
3760	468.25	590	4960	481.25	839
3800	469.0	600	5000	481.5	836
3840	469.5	606			
3880	470.0	612			
3920	470.5	618			
3960	471.25	623			
4000	472.0	628			
4040	472.5	635			
4080	473.0	639			

Comments:

APPENDIX B

Figure B1 shows a 4-wire platinum resistance thermometer (RTD) circuit including leakage and line resistances. The resistance of the RTD is denoted by R. Leakage resistances are shown between each pair of conductors in the 4-wire system, and between each conductor and the cable sheath; for simplicity, it is assumed that all these resistances have the same value r. In addition, the resistance along each of the conductors is r'. A constant current source delivering I amperes is connected across terminals $+I_k$, and $-I_k$, and the voltage E is measured with a voltmeter connected across terminals $+V_s$, and $-V_s$. A straightforward network analysis was carried out to determine how the apparent resistance $R_a = E/I$ measured at the surface differs from the actual resistance R of the RTD, as a function of the leakage and live resistances r and r'. The result is

$$R = \frac{R_a(r + 5r')^2}{r^2 + 5R_a(r + 5r')} \tag{2}$$

The problem, of course, is that the values of r and r' to use in this expression are unknown. First, the cable leakage resistance r is a function of the temperature (results of tests by Vector Cable Co.), the time at temperature (results of tests by Aerospace Research Corp.), and probably the chemical composition of fluid in which the cable is immersed. Second, the line and leakage resistances are distributed along the cable. Both depend on the borehole temperature profile, which itself is measured by the system. Third, leakage resistances at the cable head have been observed in DRI field programs, and are less predictable than the cable properties.

However, the problem can be solved "backwards"; given a specification on the temperature accuracy required, one can invert equation (2) above to determine the limiting permissible values of r and r'. The apparent resistance R_a measured at the surface will differ from the true RTD resistance R by some small value δ. The approach is then to set

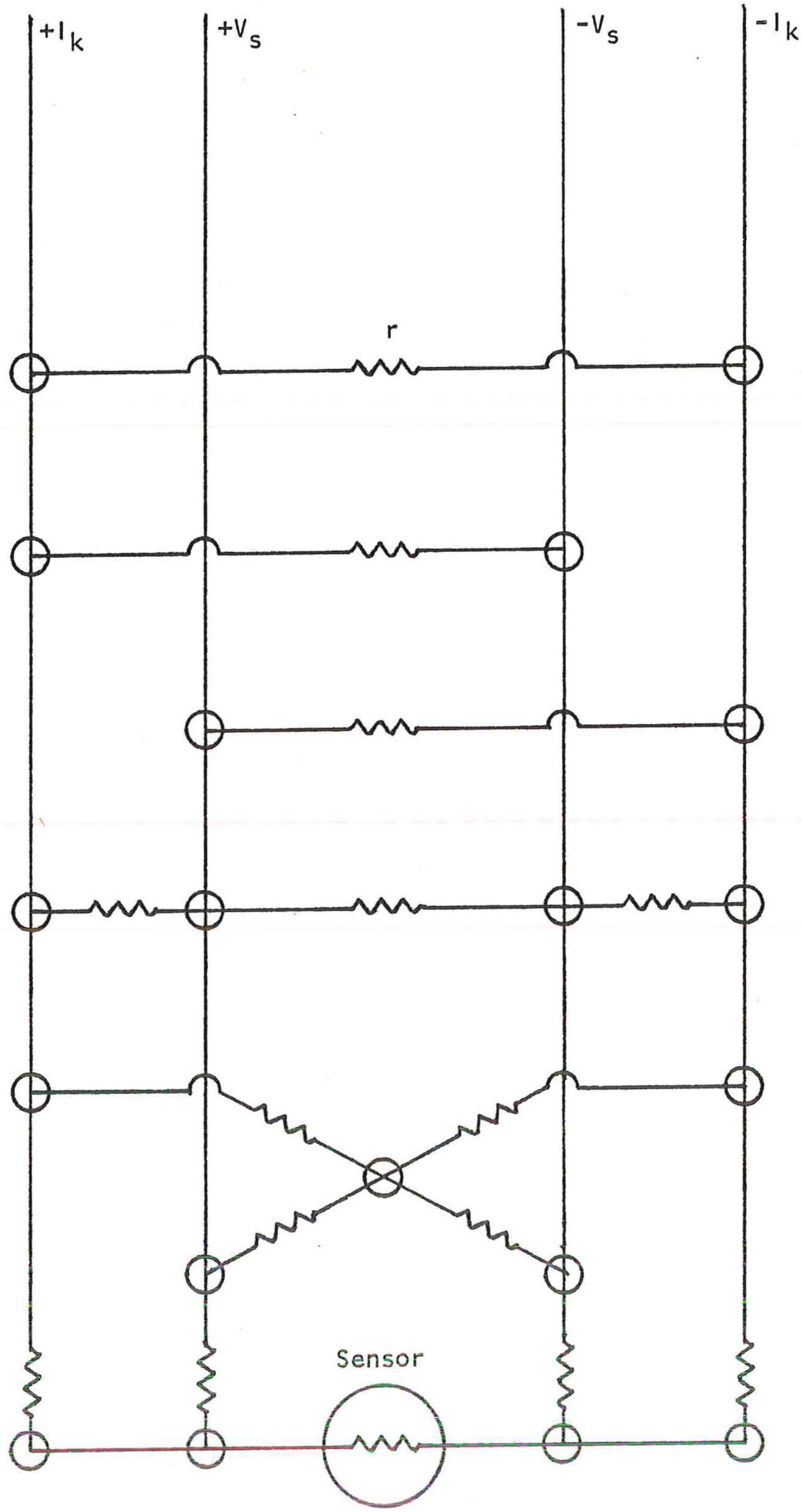

Figure B1. Leakage/Line Resistance Schematic, Four-Wire Configuration.

$R_a = R - \delta$ in equation (2), and set δ equal to the increment in the RTD resistance which corresponds to the maximum allowable error in temperature, and solve for the maximum allowable value of the leakage resistance, r_{min}:

$$r_{min} = \frac{5[(R - \delta)(R + 2r')^2 + r'\delta(R + r')]}{(R + 2r')\delta} ,$$

or, since δ is much smaller than R,

$$r_{min} \cong \frac{5R(R + 2r')}{\delta} . \qquad (3)$$

For an RTD with an ice point resistance of 100 ohms, the value of R at $500^{\circ}F$ ($260^{\circ}C$) is about 200 ohms, and dR/dT is about 0.4 ohms/deg C. For a maximum temperature error of $0.5^{\circ}C$, the solution is $\delta = 0.2$ ohm. This leads to a value of r_{min} of

$$r_{min} = \frac{5 \times 200(200 + 2r')}{0.2} = 10^6 + 10^4 r' . \qquad (4)$$

The value of the line resistance r' to be used here is considerably less than the total resistance of the logging cable. As mentioned above, the line and leakage resistances are distributed along the cable. The mathematical complexity of the circuit analysis using distributed resistances prevents a closed-form solution. However, it is obvious that only the line resistances near the RTD will contribute appreciable error to the measured temperature. This suggests that, to a first approximation, r' will be considerably less than R in the above example and can be neglected in equations (3) and (4). Thus it can be seen that the total leakage resistance between any two conductors, over the whole length of the cable, must be greater than about 1 megohm if temperature errors are to be less than, say, $0.5^{\circ}C$. Any smaller value of r will give $\delta = R - R_a > 0.2\Omega$ and a temperature error greater than $0.5^{\circ}C$.

Logging cable leakage resistances have recently been measured. The Aerospace Research Corp. immersed a 4-foot (1.2m)length of 7-conductor cable in a 5% NaCL solution at 550°F (288°C) and 7000 psig pressure for 9 hours. The resistance between each of the seven conductors and the cable sheath was measured every 15 minutes. The resistance values decreased by a factor of 30 to 100 over the 9-hour period, eventually reaching values between 0.5 and 1.8 megohms/1000 ft. (Each of the seven conductors reached a different final value.) The Vector Cable Co. measured the resistance of a 150 ft (46m) length of 7-conductor cable immersed in pure water over the temperature range from room temperature to 550°F (288°C). These references gave only one resistance value per temperature; and did not specify which conductor was used for the tests. The leakage resistance, in units of ohms/1000 ft, are given quite well by the expression,

$$R_\ell = 3.73 \times 10^{12} \exp(-0.02485T), \tag{5}$$

where temperature is in degrees F, over the range from 150° to 550°F. This leakage resistance of the entire cable in a borehole is obtained by integrating this expression over the depth of the hole, and using the measured temperature as a function of depth in the hole:

$$\frac{1}{r_\ell} = \int \frac{dx}{R_\ell[T(x)]} \ . \tag{6}$$

For a typical field test, where temperature increased approximately linearly from 450°F (232°C) to 500°F (260°C) from top to bottom in a 3000 ft (915m) deep well, this expression gives an r_ℓ value of about 8.7 megohms. The parameter r_ℓ is not the same as the parameter r in eqs. (2) and (3), however. If we assume that there is leakage between each of the 7 conductors in the cable and its nearest neighbor, as well as between each conductor and the cable sheath, then the leakage between each conductor and the cable sheath consists of the direct leakage to the sheath plus the leakage through each of the alternative leakage paths through the other conductors and thence to the sheath. The leakage resistance network is then shown in Figure B2. The measured leakage

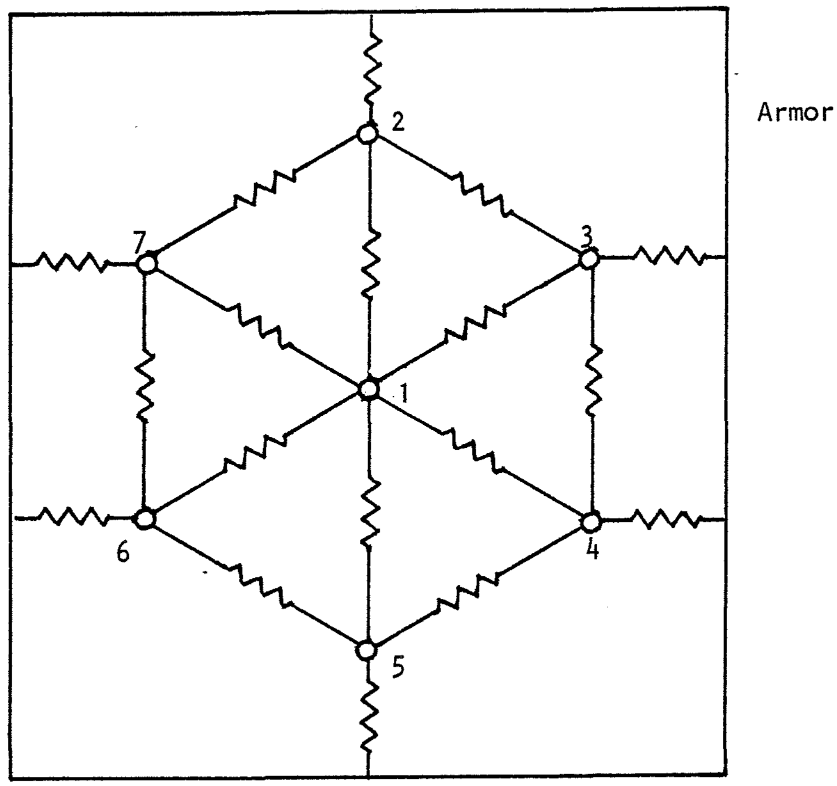

Figure B2. Leakage Resistance Model, Seven Conductor Logging Cable.

resistance r_ℓ is related to the individual leakage element r in this network by

$$r \cong 2.7 r_\ell \qquad \text{for conductors 1 through 6}$$

$$r = 3 r_\ell \qquad \text{for conductor 7}$$

Thus for the example given above, the value of r is $2.7 \times 8.7 \times 10^6 = 23$ megohms. In this case, then, cable leakages would not lead to appreciable temperature errors. Going up in temperature by another $50^\circ F$ ($28^\circ C$) decreases the leakage resistance by almost a factor of four, however. Moreover, holding at this temperature for several hours can reduce the leakage resistance by another factor of four, approximately as measured in the Aerospace Research Corp. tests, which puts cable leakage resistance right on the borderline so far as the specified temperature accuracy is concerned.

The greatest problem, however, seems to be the cable head. In at least one field experiment, leakage resistances between two conductors (shorted together) and the sheath were measured as low as 35K ohms. (Marked deterioration of the cable head connector was noted in these tests, suggesting strongly that the leakage was in the cable head and not the cable itself.) This corresponds to an r value, in eq. (2), of about 100 k ohms, and thus suggests that measured temperatures could have been in error by approximately $10^\circ F$, or $5^\circ C$, in tests with this system. The leakage resistances measured during the field tests were definitely inversely proportional to exposed length of cable, so that the error noted above is a maximum at maximum depth of measurement, approximately 6060 ft (1850m). Leakage resistance at the suspected production horizon were much higher than that measured at the maximum depth, with a projected error of 2 to $4^\circ F$ (1 to $2^\circ C$). It must be noted here that logging data listed in the tables and shown on graphs in this report, are raw values since there was not sufficient information concerning the leakage phenomenon to develop a correction scheme.